

Convergence Rate Bounds for the Mirror Descent Method: IQCs, Popov Criterion and Bregman Divergence [★]

Mengmou Li ^{a,b}, Khaled Laib ^{a,d}, Takeshi Hatanaka ^c, Ioannis Lestas ^a

^a*Department of Engineering, University of Cambridge, Trumpington Street, Cambridge CB2 1PZ, United Kingdom (email: mml.research@gmail.com; kl507@cam.ac.uk; icl20@cam.ac.uk).*

^b*Graduate School of Advanced Science and Engineering, Hiroshima University, 1-2-1 Kagamiyama, Higashi-Hiroshima, Japan (email: mengmou@hiroshima-u.ac.jp).*

^c*Department of Systems and Control Engineering, School of Engineering, Tokyo Institute of Technology, S5-16, 2-12-1 Ookayama, Meguro-ku, Tokyo, Japan (email: hatanaka@sc.e.titech.ac.jp).*

^d*School of Engineering, University of Leicester, Leicester, LE1 7RH, United Kingdom (email: kl314@le.ac.uk).*

Abstract

This paper presents a comprehensive convergence analysis for the mirror descent (MD) method, a widely used algorithm in convex optimization. The key feature of this algorithm is that it provides a generalization of classical gradient-based methods via the use of generalized distance-like functions, which are formulated using the Bregman divergence. Establishing convergence rate bounds for this algorithm is in general a non-trivial problem due to the lack of monotonicity properties in the composite nonlinearities involved. In this paper, we show that the Bregman divergence from the optimal solution, which is commonly used as a Lyapunov function for this algorithm, is a special case of Lyapunov functions that follow when the Popov criterion is applied to an appropriate reformulation of the MD dynamics. This is then used as a basis to construct an integral quadratic constraint (IQC) framework through which convergence rate bounds with reduced conservatism can be deduced. We also illustrate via examples that the convergence rate bounds derived can be tight.

Key words: Mirror descent method, Bregman divergence function, convergence rate, Popov criterion, integral quadratic constraints, linear matrix inequalities

1 Introduction

The mirror descent (MD) method was initially proposed by Nemirovskij & Yudin (1983) for solving constrained convex optimization problems. By choosing a Bregman distance function in place of the Euclidean distance to reflect the geometry of the constraint sets, it generalizes the gradient descent (GD) method from the Euclidean space to Hilbert and Banach spaces (Bubeck et al. (2015)). Attempts have been made to unify or incorporate the MD method with various algorithms, such as the nonlinear projected subgradient algorithms (Beck & Teboulle (2003)), online learning algorithms (Raskutti & Mukherjee (2015)), accelerated algorithms (Krichene et al. (2015), Wibisono et al. (2016)), and dual averaging (Juditsky et al. (2022)). Due to its applicability in non-Euclidean space, it has received considerable re-

search attention in many contexts, such as stochastic optimization (Duchi et al. (2012), Nedic & Lee (2014), Borovykh et al. (2022)), distributed optimization (Yuan et al. (2018), Doan et al. (2018), Sun et al. (2022)), and machine learning (Mertikopoulos et al. (2018)).

In contrast to the abundant literature on well-known algorithms such as gradient descent and Nesterov's accelerated algorithms, there is a lack of references characterizing a tight bound on the convergence rate for the MD method with a constant stepsize. While Lu et al. (2018) adopt the notion of relative smoothness/convexity and Sun et al. (2022) use Lyapunov functions formulated via quadratic constraints (QCs), respectively, to obtain convergence rate bounds for the MD method under a constant stepsize, these bounds are not tight in general. It is important to address these problems, as diminishing stepsizes usually lead to slower convergence than constant stepsizes, and tight convergence rate bounds are crucial in the analysis and

[★] A preliminary version of this paper was presented in the 61st IEEE Conference on Decision and Control (CDC 2022).

applications of optimization algorithms.

When bounds on the convergence rate need to be established, it is important to have systematic methods that allow to construct Lyapunov functions with more advanced structures, or allow via other means to deduce convergence rates with reduced conservatism. It has been pointed out in the optimization literature that integral quadratic constraint (IQC) framework (Megretski & Rantzer (1997)) can be a useful tool in this direction (Lessard et al. (2016), Dhingra et al. (2018), Scherer et al. (2023)). However, there has been no application of IQCs to the case of MD algorithm, as the MD dynamics involve the composition of two nonlinearities that correspond to monotone operators, with this composition not preserving these monotonicity properties.

In the analysis of MD algorithm, the commonly used Lyapunov function is the Bregman divergence function representing a generalized distance between the decision variable and the optimal solution. The Bregman divergence function was introduced by Bregman (1967) to find the intersection of convex sets. It has had applications in the analysis of distributed optimization (Li et al. (2020)), port-Hamiltonian systems (Jayawardhana et al. (2007)), equilibrium independent stability (Simpson-Porco (2018)), and power systems (De Persis & Monshizadeh (2017), Monshizadeh & Lestas (2019)), in addition to the analysis of the MD algorithm.

Despite the nice geometric interpretation of the Bregman divergence in the context of the MD method, no link has been established thus far between the use of the Bregman divergence from the optimal solution as a Lyapunov function and robustness analysis tools. Such connections are important as they can motivate wider classes of multipliers through which less conservative convergence rate bounds can be established.

One of our main contributions in this manuscript is to show that there is indeed such an inherent connection, whereby the Bregman-based Lyapunov function for the MD method is a special case of Lyapunov functions that follow when the Popov criterion is appropriately applied. The problem formulation that leads to this result can therefore be used as a basis to develop an IQC framework for establishing improved rate bounds for the MD method.

Our contributions in this paper can be summarized as follows:

- i) We show that the use of the Bregman divergence from the optimal solution as a Lyapunov function for the continuous-time MD method is a special case of Lyapunov functions that follow from the Popov criterion, when this is applied to an appropriate reformulation of the MD dynamics.
- ii) We use the reformulation of the MD dynamics that leads to the result above to develop an IQC framework for deriving convergence rate bounds. We employ conic combinations of Popov IQCs and other types of IQCs to derive convergence rate bounds for the discrete-time MD method. These bounds are less conservative than the current state of the art

- and their tightness is also illustrated via examples.
- iii) We also extend our results to the case of the projected MD algorithm, where projections are additionally included in the dynamics. A framework is provided for establishing convergence rate bounds for the projected MD method with a constant step-size. In particular, the convergence rate is analyzed via additional IQCs associated with the projection operator and the repeated nonlinearities formulated.

The convergence rate bounds deduced are formulated as solutions to linear matrix inequalities (LMIs) in both discrete and continuous time. Compared to the preliminary version of this paper Li et al. (2022), we obtain an analytical expression for the largest convergence rate bound in continuous time, and include the complete proofs of the convergence analysis for the unconstrained MD algorithm. Moreover, we analyze the convergence rate of the projected MD algorithm.

The rest of this paper is organized as follows. In Section 2, preliminaries on the MD method and IQCs are provided. The continuous-time and discrete-time MD methods are analyzed via IQCs in Section 3 and Section 4, respectively. In addition, the projected variant of the discrete-time MD algorithm is analysed in Section 5. In Section 6, numerical examples are given to verify our results. Finally, the paper is concluded in Section 7.

2 Preliminaries

2.1 Notation

Let \mathbb{R} , \mathbb{Z} , and \mathbb{Z}_+ denote the set of real numbers, integers, and nonnegative integers, respectively. Let I_d and 0_d denote the $d \times d$ identity matrix and zero matrix, respectively. Their subscripts can be omitted if it is clear from the context. The notation $\text{diag}(\alpha_1, \dots, \alpha_d)$ denotes a $d \times d$ diagonal matrix with α_i on its i -th diagonal entry. Let \mathbf{RH}_∞ be the set of proper real rational functions without poles in the closed right-half plane. The set of $m \times n$ matrices with elements in \mathbf{RH}_∞ is denoted $\mathbf{RH}_\infty^{m \times n}$. Let $\mathbf{L}_2^m[0, \infty)$ be the Hilbert space of all square integrable and Lebesgue measurable functions $f : [0, \infty) \rightarrow \mathbb{R}^m$. It is a subspace of $\mathbf{L}_{2e}^m[0, \infty)$ whose elements only need to be integrable on finite intervals. Let $l_2^m(\mathbb{Z}_+)$ be the set of all square summable sequences $f : \mathbb{Z}_+ \rightarrow \mathbb{R}^m$. Given a Hermitian matrix $H(j\omega)$, $H^*(j\omega) := H^T(-j\omega)$ represents its conjugate transpose and $\{H(j\omega)\}_H := \frac{1}{2}(H(j\omega) + H^*(j\omega))$ denotes its Hermitian part. For a vector $x \in \mathbb{R}^n$ we denote by $x^{(k)}$ its k -th element.

Given a set \mathcal{X} , $\text{int}\mathcal{X}$ denotes the interior of \mathcal{X} and $\text{bd}\mathcal{X}$ denotes the boundary of \mathcal{X} . The normal cone of \mathcal{X} at a point $x \in \mathcal{X}$ is defined by $N_{\mathcal{X}}(x) = \{v : \langle v, y - x \rangle \leq 0, \forall y \in \mathcal{X}\}$.

Given $0 \leq \mu \leq L$, we denote $S(\mu, L)$ as the set of functions $f : \mathbb{R}^d \rightarrow \mathbb{R}$ that are continuously differentiable, μ -strongly convex and L -smooth, i.e., $\forall x, y$,

$$\mu\|x - y\|^2 \leq (\nabla f(x) - \nabla f(y))^T (x - y) \leq L\|x - y\|^2.$$

In this work, we assume $\mu > 0$ for all the functions we study if not specified otherwise. The condition number κ of functions in $S(\mu, L)$ is defined by $\kappa := L/\mu \geq 1$.

A memoryless nonlinearity $\psi : \mathbb{R} \rightarrow \mathbb{R}$, $\psi(0) = 0$, is said to be *sloped-restricted* on sector $[\alpha, \beta]$, if $\alpha \leq \frac{\psi(x) - \psi(y)}{x - y} \leq \beta$, for all $x \neq y$ and $x, y \in \mathbb{R}$.

2.2 Integral quadratic constraints

To facilitate readability some preliminaries on integral quadratic constraints (Rantzer (1996), Jönsson (2001)) are included in this section.

In continuous time, a bounded operator $\Delta : \mathbf{L}_2^n[0, \infty) \rightarrow \mathbf{L}_2^m[0, \infty)$ is said to satisfy the IQC defined by Π , denoted by $\Delta \in \text{IQC}(\Pi)$, if

$$\int_{-\infty}^{\infty} \begin{bmatrix} \hat{v}(j\omega) \\ \hat{w}(j\omega) \end{bmatrix}^* \Pi(j\omega) \begin{bmatrix} \hat{v}(j\omega) \\ \hat{w}(j\omega) \end{bmatrix} d\omega \geq 0 \quad (1)$$

for all $v \in \mathbf{L}_2^n[0, \infty)$ and $w = \Delta(v)$, where $\hat{v}(j\omega)$, $\hat{w}(j\omega)$ are the Fourier transforms of v , w , respectively, and $\Pi(j\omega)$ can be any measurable Hermitian valued function. In discrete time, condition (1) reduces to

$$\int_{-\pi}^{\pi} \begin{bmatrix} \hat{v}(e^{j\omega}) \\ \hat{w}(e^{j\omega}) \end{bmatrix}^* \Pi(e^{j\omega}) \begin{bmatrix} \hat{v}(e^{j\omega}) \\ \hat{w}(e^{j\omega}) \end{bmatrix} d\omega \geq 0$$

for all $v \in l_2^n(\mathbb{Z}_+)$, and $w = \Delta(v)$, where $\hat{v}(e^{j\omega})$, $\hat{w}(e^{j\omega})$ represent the discrete-time Fourier transform of v , w respectively.

Define the truncation operator P_T which does not change a function on the interval $[0, T]$ and gives the value zero on $(T, \infty]$. The operator Δ is said to be *causal* if $P_T \Delta P_T = P_T \Delta$, for all $T \geq 0$. Consider the interconnection

$$\begin{aligned} v &= Gw + g \\ w &= \Delta(v) + e \end{aligned} \quad (2)$$

where $g \in \mathbf{L}_{2e}^l[0, \infty)$, $e \in \mathbf{L}_{2e}^m[0, \infty)$, G and Δ are two causal operators on $\mathbf{L}_{2e}^m[0, \infty)$, $\mathbf{L}_{2e}^l[0, \infty)$, respectively. It is assumed that G is a stable linear time-invariant operator and Δ has bounded gain denoted as $\|\Delta\|$. The feedback interconnection of G and Δ is *well-posed* if the map $(v, w) \mapsto (e, g)$ defined by (2) has a causal inverse on $\mathbf{L}_{2e}^{m+l}[0, \infty)$. The interconnection is *stable* if, in addition, the inverse is bounded, i.e., there exists a constant $c > 0$ such that $\int_0^T (|v|^2 + |w|^2) dt \leq c \int_0^T (|g|^2 + |e|^2) dt$. System (2) with linear G and static nonlinear Δ is called the *Lur'e system*.

We adopt the following IQC theorem for analysis.

Theorem 1 (Megretski & Rantzer (1997)) *Let $G(s) \in \mathbf{RH}_{\infty}^{l \times m}$, and let Δ be a bounded causal operator. Assume that:*

- (1) *for every $\tau \in [0, 1]$, the interconnection of G and $\tau\Delta$ is well-posed;*
- (2) *for every $\tau \in [0, 1]$, the IQC defined by Π is satisfied by $\tau\Delta$;*

(3) *there exists $\epsilon > 0$ such that*

$$\begin{bmatrix} G(j\omega) \\ I \end{bmatrix}^* \Pi(j\omega) \begin{bmatrix} G(j\omega) \\ I \end{bmatrix} \leq -\epsilon I, \quad \forall \omega \in \mathbb{R}. \quad (3)$$

Then, the interconnection of G and Δ is stable.

Remark 1 *If $\Pi(j\omega) = \begin{bmatrix} \Pi_{11}(j\omega) & \Pi_{12}(j\omega) \\ \Pi_{12}^*(j\omega) & \Pi_{22}(j\omega) \end{bmatrix}$ satisfies*

$\Pi_{11}(j\omega) \geq 0$ and $\Pi_{22}(j\omega) \leq 0$, then the condition $\Delta \in \text{IQC}(\Pi)$ implies that $\tau\Delta \in \text{IQC}(\Pi)$ for all $\tau \in [0, 1]$. $\Pi(j\omega)$ in Megretski & Rantzer (1997) is required to be essentially bounded, and extensions that allow to include also the Popov IQC were derived in Jönsson (1997).

The IQC theorem for discrete-time systems can be found in, e.g., Jönsson (2001).

2.3 Mirror descent algorithm

Consider the optimization problem

$$\min_{x \in \mathcal{X}} f(x) \quad (4)$$

where \mathcal{X} is a closed and convex constraint set and $\mathcal{X} \subseteq \mathbb{R}^d$, f is the objective function and $f \in S(\mu, L)$. We will consider the unconstrained case in Section 3, and 4 first, i.e., $\mathcal{X} = \mathbb{R}^d$, and the constrained case in Section 5.

When $\mathcal{X} = \mathbb{R}^d$, we can solve (4) with the well-known gradient descent (GD) algorithm $x_{k+1} = x_k - \eta \nabla f(x_k)$, or equivalently,

$$x_{k+1} = \operatorname{argmin}_{x \in \mathbb{R}^d} \left\{ \nabla f(x_k)^T x + \frac{1}{2\eta} \|x - x_k\|_2^2 \right\}$$

where $\eta > 0$ is a fixed stepsize. Observe that the Euclidean norm used above can be replaced by other distance measures to generate new algorithms.

The *Bregman divergence* defined with respect to a distance generating function (DGF) $\phi : \mathbb{R}^d \rightarrow \mathbb{R}$ is given by

$$D_{\phi}(y, x) = \phi(y) - \phi(x) - (y - x)^T \nabla \phi(x). \quad (5)$$

where $\phi(x) \in S(\mu_{\phi}, L_{\phi})$. Then, the MD algorithm is given by

$$x_{k+1} = \operatorname{argmin}_{x \in \mathbb{R}^d} \left\{ \nabla f(x_k)^T x + \frac{1}{\eta} D_{\phi}(x, x_k) \right\}. \quad (6)$$

When $\phi(x) = \frac{1}{2} \|x\|^2$, the MD algorithm is reduced to the GD algorithm. Denote $\bar{\phi}$ as the convex conjugate of function ϕ , i.e.,

$$\bar{\phi}(z) = \sup_{x \in \mathbb{R}^d} \{x^T z - \phi(x)\}. \quad (7)$$

Denote $\mu_{\bar{\phi}} = (L_{\phi})^{-1}$, and $L_{\bar{\phi}} = (\mu_{\phi})^{-1}$. It follows from (Rockafellar & Wets 2009, Proposition 11.3 and 12.60)

that $\bar{\phi} \in S(\mu_{\bar{\phi}}, L_{\bar{\phi}})$, and $z = \nabla\phi(x) \iff x = \nabla\bar{\phi}(z)$. In other words, $\nabla\bar{\phi}$ is the inverse function of $\nabla\phi$. Then, from the optimality condition for the right-hand side of (6), the MD algorithm can be written as

$$z_{k+1} = z_k - \eta \nabla f(x_k), \quad x_{k+1} = \nabla\bar{\phi}(z_{k+1})$$

or equivalently,

$$z_{k+1} = z_k - \eta(\nabla f \circ \nabla\bar{\phi})(z_k) \quad (8)$$

where \circ represents composition of functions. Similarly, the continuous-time MD algorithm can be given by

$$\dot{z}(t) = -\eta(\nabla f \circ \nabla\bar{\phi})(z(t)). \quad (9)$$

Any equilibrium point of the above systems satisfies $\nabla f(\nabla\bar{\phi}(z^{\text{opt}})) = \nabla f(x^{\text{opt}}) = 0_d$, which yields the optimal solution to problem (4). In the remainder of this paper, the time argument in the continuous-time case will be omitted to simplify the notation.

Note that the DGF ϕ can be an arbitrary function in $S(\mu_{\phi}, L_{\phi})$. Function ϕ is usually chosen such that its convex conjugate is easily computable. One of the motivations in the choice of ϕ is to generate a distance function that reflects the geometry of the given constraint set \mathcal{X} so that projections in \mathcal{X} can be avoided¹ during the implementation of the algorithm. For example, choosing the negative entropy $\phi(x) = \sum_{i=1}^d x^{(i)} \ln x^{(i)}$ avoids the direct use of projection when considering minimization over the unit simplex $\mathcal{X} = \{x = [x^{(1)}, \dots, x^{(d)}]^T \in \mathbb{R}_+^d : \sum_{i=1}^d x^{(i)} = 1\}$ (Beck & Teboulle (2003), Bubeck et al. (2015)). Additionally, the choice of ϕ changes the geometry of gradient descent, potentially improving the convergence rate (Maddison et al. (2021)).

3 Continuous-time mirror descent method

We start our discussion in this paper with the analysis of the continuous-time MD method. A main result in this section is to reveal a connection between the Bregman divergence and the Popov criterion when these are used as tools for stability analysis. In particular, we show that the use of the Bregman divergence from the optimal solution as a Lyapunov function, is a special case of Lyapunov functions that follow from the Popov criterion when it is applied to an appropriate reformulation of the MD dynamics. This connection is used as a basis to develop an IQC framework that can provide convergence rate bounds with reduced conservatism. In particular, this framework is exploited in subsequent sections to provide convergence rate bounds in a discrete-time setting and also when projections are considered to constrain the dynamics in prescribed sets.

¹ In particular, projections in \mathcal{X} are avoided when condition (33) stated in Section 5.1 is satisfied (Beck & Teboulle (2003)).

3.1 MD algorithm in the form of Lur'e systems

The composition of operators in (9) hinders the direct application of an IQC framework since the composite operator may not belong to the original classes of the two operators, e.g., the composition of two monotone operators is not necessarily monotone. Nevertheless, the cascade connection of two nonlinear operators can be transformed into the feedback interconnection of a linear system with the direct sum of the two nonlinear operators, similarly to the example in Megretski & Rantzer (1997). Thus, (9) can be written into a Lur'e system

$$\dot{z} = -\eta u'_1, \quad u'_1 = \nabla f(y_1), \quad y_1 = u'_2, \quad u'_2 = \nabla\bar{\phi}(y_2), \quad y_2 = z.$$

Moreover, we would like to transform the nonlinearities into sector-bounded ones that allow to generate IQCs that fulfil the second condition in Theorem 1 (discussed in Section 3.2.1). Therefore, the continuous-time MD algorithm (9) is rewritten as

$$\dot{z} = Az + Bu, \quad y = Cz + Du \quad (10)$$

where $u = \begin{bmatrix} u_1 \\ u_2 \end{bmatrix}$, $y = \begin{bmatrix} y_1 \\ y_2 \end{bmatrix}$, the system matrices are

$$\begin{bmatrix} A & B \\ C & D \end{bmatrix} = \begin{bmatrix} -\eta\mu_f\mu_{\bar{\phi}}I_d & -\eta I_d - \eta\mu_f I_d \\ \mu_{\bar{\phi}}I_d & 0_d & I_d \\ I_d & 0_d & 0_d \end{bmatrix} \quad (11)$$

and the system input is

$$\begin{bmatrix} u_1 \\ u_2 \end{bmatrix} = \begin{bmatrix} \nabla f(y_1) - \mu_f y_1 \\ \nabla\bar{\phi}(y_2) - \mu_{\bar{\phi}} y_2 \end{bmatrix}. \quad (12)$$

The transfer function matrix of the linear system is

$$\begin{aligned} G(s) &= C(sI_d - A)^{-1}B + D \\ &= \frac{1}{s + \eta\mu_f\mu_{\bar{\phi}}} \begin{bmatrix} -\eta\mu_{\bar{\phi}} & s \\ -\eta & -\eta\mu_f \end{bmatrix} \otimes I_d \end{aligned} \quad (13)$$

where \otimes denotes the Kronecker product. Next, we define $z^{\text{opt}}, x^{\text{opt}}$ as the unique optimal state with corresponding variables y^{opt} and u^{opt} . Let $\tilde{z} = z - z^{\text{opt}}$, $\tilde{y} = y - y^{\text{opt}}$, $\tilde{u} = u - u^{\text{opt}}$. We obtain the error system

$$\dot{\tilde{z}} = A\tilde{z} + B\tilde{u}, \quad \tilde{y} = C\tilde{z} + D\tilde{u} \quad (14)$$

with

$$\tilde{u} := \Delta \left(\begin{bmatrix} y_1 - y_1^{\text{opt}} \\ y_2 - y_2^{\text{opt}} \end{bmatrix} \right) = \begin{bmatrix} \Delta_1 (y_1 - y_1^{\text{opt}}) \\ \Delta_2 (y_2 - y_2^{\text{opt}}) \end{bmatrix}, \quad (15)$$

where $\Delta_1(x)$, $\Delta_2(x)$ are defined by $\Delta_1(x) = (\nabla f(x + y_1^{\text{opt}}) - \mu_f(x + y_1^{\text{opt}})) - (\nabla f(y_1^{\text{opt}}) - \mu_f y_1^{\text{opt}})$, $\Delta_2(x) = (\nabla \bar{\phi}(x + y_2^{\text{opt}}) - \mu_{\bar{\phi}}(x + y_2^{\text{opt}})) - (\nabla \bar{\phi}(y_2^{\text{opt}}) - \mu_{\bar{\phi}} y_2^{\text{opt}})$. The above error system is in the form of a Lur'e system (2), where $v = \tilde{y}$, $w = \tilde{u}$, $e = 0_d$, and g is a trajectory that represents the effect of the initial condition. The transformation is illustrated in Fig. 1.

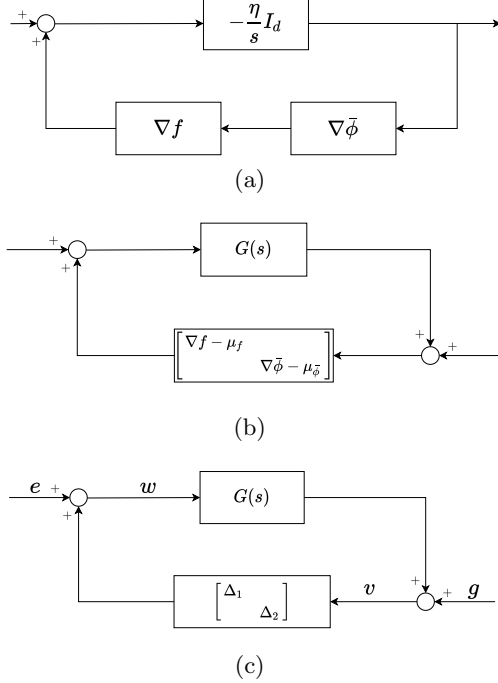


Fig. 1. Transformation of the MD method to a Lur'e system. (a) represents the composition of operators, which is transformed to the direct sum of operators in (b), where $G(s)$ is given by (13). (c) is the error system in (14), and Δ_1 , Δ_2 are given by (15).

3.2 IQCs for gradients of convex functions

In this subsection, we will include a number of useful IQCs for the gradients of convex functions so as to characterize the nonlinearity Δ . Note that conic combinations of various IQCs are also valid IQCs which better characterize the nonlinearity and lead to less conservative stability margins.

3.2.1 Sector IQC

The Sector IQC stated in the following lemma is a result of the co-coercivity of gradients.

Lemma 1 (Lessard et al. (2016)) Suppose $f \in S(\mu_f, L_f)$. For all x, y , the following quadratic constraint (QC) is satisfied,

$$\begin{bmatrix} y-x \\ \nabla f(y) - \nabla f(x) \end{bmatrix}^T \begin{bmatrix} -2\mu_f L_f I_d & (L_f + \mu_f) I_d \\ (L_f + \mu_f) I_d & -2I_d \end{bmatrix} \begin{bmatrix} y-x \\ \nabla f(y) - \nabla f(x) \end{bmatrix} \geq 0.$$

Note that as $f \in S(\mu_f, L_f)$, $\bar{\phi} \in S(\mu_{\bar{\phi}}, L_{\bar{\phi}})$, then $f(\cdot) - \frac{1}{2}\mu_f \|\cdot\|^2 \in S(0, L_f - \mu_f)$ and $\bar{\phi}(\cdot) - \frac{1}{2}\mu_{\bar{\phi}} \|\cdot\|^2 \in$

$S(0, L_{\bar{\phi}} - \mu_{\bar{\phi}})$. Moreover, using Lemma 1, we have that, given Δ defined in (15), $\Delta \in \text{IQC}(\Pi_s)$, where

$$\Pi_s = \begin{bmatrix} 0_d & 0_d & \alpha_1(L_f - \mu_f)I_d & 0_d \\ 0_d & 0_d & 0_d & \alpha_2(L_{\bar{\phi}} - \mu_{\bar{\phi}})I_d \\ \alpha_1(L_f - \mu_f)I_d & 0_d & -2\alpha_1 I_d & 0_d \\ 0_d & \alpha_2(L_{\bar{\phi}} - \mu_{\bar{\phi}})I_d & 0_d & -2\alpha_2 I_d \end{bmatrix} \quad (16)$$

for some $\alpha_1, \alpha_2 \geq 0$. The second condition in Theorem 1 is always satisfied with this IQC.

3.2.2 Popov IQC

The Popov IQC can be stated as follows.

Lemma 2 (Jönsson (1997)) Suppose $f \in S(0, L)$. The nonlinearity $\nabla f(x) - \nabla f(x^{\text{opt}})$ satisfies the Popov IQC defined by the multiplier

$$\Pi_P(j\omega) = \pm \begin{bmatrix} 0_d & -j\omega I_d \\ j\omega I_d & 0_d \end{bmatrix}$$

in the sense described in (Jönsson 1997, Definition 1). As $f(\cdot) - \frac{1}{2}\mu_f \|\cdot\|^2 \in S(0, L_f - \mu_f)$ and $\bar{\phi}(\cdot) - \frac{1}{2}\mu_{\bar{\phi}} \|\cdot\|^2 \in S(0, L_{\bar{\phi}} - \mu_{\bar{\phi}})$, using Lemma 2, we have $\Delta \in \text{IQC}(\Pi_p)$, where Δ is defined in (15) and

$$\Pi_p(j\omega) = \begin{bmatrix} 0_d & 0_d & -j\omega\beta_1 I_d & 0_d \\ 0_d & 0_d & 0_d & -j\omega\beta_2 I_d \\ j\omega\beta_1 I_d & 0_d & 0_d & 0_d \\ 0_d & j\omega\beta_2 I_d & 0_d & 0_d \end{bmatrix} \quad (17)$$

for some $\beta_1, \beta_2 \in \mathbb{R}$.

It is worth noting that the nonlinearity $\nabla f(x) - \nabla f(x^{\text{opt}})$ with $f \in S(0, L)$ satisfies the IQC defined by $\Pi(j\omega)$ given by

$$\Pi(j\omega) = \begin{bmatrix} 0_d & M^*(j\omega)I_d \\ M(j\omega)I_d & 0_d \end{bmatrix} \quad (18)$$

where $M(j\omega) = 1 - H(j\omega)$ and $H(j\omega)$ is the Fourier transform of any signal $h(t)$ such that $h(t) \geq 0$ and $\int_{-\infty}^{+\infty} |h(t)|dt \leq 1$. These $M(j\omega)$ are known as the Zames-Falb-O'Shea multipliers. It is well-known that the Zames-Falb-O'Shea multipliers can be used to formulate a wide class of IQCs that are satisfied by slope-restricted nonlinearities (see also the discrete-time analogues in Lessard et al. (2016) formulated in time domain).

Remark 2 The Popov IQC can be obtained by letting $M(j\omega) = j\omega$ in (18). Note that the Popov multipliers are not Zames-Falb-O'Shea multipliers since the resulting $H(j\omega) = 1 - M(j\omega)$ is unbounded. Nevertheless, the Popov multipliers can be treated as a limit to the first order Zames-Falb-O'Shea multipliers² (Carrasco et al. (2013)).

² We will show later on that conic combinations of Sector and Popov IQCs can recover the Bregman divergence based Lyapunov function in continuous time. The discrete-time analogues of Zames-Falb-O'Shea multipliers could be bene-

3.3 Convergence analysis via IQCs in frequency domain

In this subsection, we will present a convergence analysis for the continuous-time MD method. There exists rich literature showing the convergence of the MD method, e.g., Nemirovskij & Yudin (1983), Beck & Teboulle (2003), Krichene et al. (2015). Our approach using an IQC analysis framework recovers known conclusions of convergence, but also lays the foundation for the subsequent sections where tight bounds on the convergence rate are obtained in discrete time. Furthermore, it allows to consider the more involved problem where projections to a convex set are additionally included.

Theorem 2 *The Lur'e system described by (2) where $g \in \mathbf{L}_2[0, \infty)$, $e \in \mathbf{L}_2[0, \infty)$, $G(s)$ is given by (13), Δ is defined in (15) with $f \in S(\mu_f, L_f)$, $\phi \in S(\mu_\phi, L_\phi)$, is stable. Furthermore, the trajectory of $x = \nabla \bar{\phi}(z)$ with any initial condition $z(0) = z_0$ of the MD algorithm (9) converges to the optimal solution of problem (4).*

PROOF. See Appendix A.

The proof of Theorem 2 can be seen as an application of the multivariable Popov criterion, which is adapted below from Moore & Anderson (1968), Khalil (2002), Jönsson (1997), Carrasco et al. (2013).

Lemma 3 *Let $H(s) \in \mathbf{RH}_\infty^{p \times p}$ and let $\psi : \mathbb{R}^p \rightarrow \mathbb{R}^p$, $\psi(0) = 0$, be a memoryless nonlinearity composed of p memoryless nonlinearities ψ_i with each being slope-restricted on sector $[0, k_i]$, i.e., $0 \leq \frac{\psi_i(x_1) - \psi_i(x_2)}{x_1 - x_2} \leq k_i$, $\forall x_1 \neq x_2$, $0 < k_i \leq \infty$, for $1 \leq i \leq p$. If there exist constants $q_i \geq 0$ and $\gamma_i \geq 0$ such that $\{QK^{-1} + (Q + j\omega\Gamma)H(j\omega)\}_H \geq \delta I$, $\forall \omega \in \mathbb{R}$, for some $\delta > 0$, where $K = \text{diag}(k_1, \dots, k_p)$, $Q = \text{diag}(q_1, \dots, q_p)$, $\Gamma = \text{diag}(\gamma_1, \dots, \gamma_p)$, and $\Gamma H(\infty) = 0$, then the negative feedback interconnection of $H(s)$ and ψ is stable.*

Remark 3 *The third condition in Theorem 1, with the IQC used in the proof of Theorem 2, is equivalent to the frequency domain inequality condition in Lemma 3 with $H(s) = -G(s)$. The consideration of different parameters q_i is crucial since it provides more flexibility and thus less conservative results for the MIMO case (Moore & Anderson (1968)). The original Popov criterion requires that the stable linear system $H(s)$ is strictly proper (Moore & Anderson (1968), Khalil (2002)). This restriction is relaxed to $\Gamma H(\infty) = 0$ in Jönsson (1997).*

Theorem 2 is based on conditions in frequency domain, which do not describe the convergence rate of the MD algorithm. To this end, we will investigate, in the next subsection, the MD method in time domain.

fictional in discrete time to reduce the conservatism, or when projections are additionally included.

3.4 Convergence rate analysis via IQCs in time domain

In this subsection, we analyze convergence rate of the MD algorithm. Moreover, we show that the Bregman divergence function, which is widely used as a Lyapunov function for the MD algorithm, is a special case of Lyapunov functions that are associated with the Popov criterion.

We can combine Theorem 2 with what is proposed in Hu & Seiler (2016) to obtain a condition that leads to lower bounds on the exponential convergence rate for the continuous-time MD method. A continuous-time signal $x(t)$ converges to x^{opt} exponentially with rate $\rho > 0$ if there exists $c > 0$ such that $\|x(t) - x^{\text{opt}}\| \leq ce^{-\rho t} \|x(0) - x^{\text{opt}}\|$, $\forall t \geq 0$.

Theorem 3 *The continuous-time MD algorithm (9) with $f \in S(\mu_f, L_f)$, $\phi \in S(\mu_\phi, L_\phi)$, converges exponentially to the optimal solution with rate ρ if there exist $P = P^T > 0$, $\Gamma = \text{diag}(0, \gamma) \geq 0$, and $Q = \text{diag}(q_1, q_2) \geq 0$ such that*

$$\begin{bmatrix} P\tilde{A}_\rho + \tilde{A}_\rho^T P & P\tilde{B} - \tilde{C}_\rho^T \\ * & -(\tilde{D} + \tilde{D}^T) \end{bmatrix} \leq 0 \quad (19)$$

where $\tilde{A}_\rho = A + \rho I$, $\tilde{B} = -B$, $\tilde{C}_\rho = (Q + 2\rho\Gamma)C + \Gamma CA$, $\tilde{D} = -QD + QK^{-1} - \Gamma CB$, $K = \text{diag}(L_f - \mu_f, L_\phi - \mu_\phi)$, and (A, B, C, D) is defined in (11). Moreover, the largest lower bound on the convergence rate for any $f \in S(\mu_f, L_f)$, $\phi \in S(\mu_\phi, L_\phi)$ is given by $\rho = \eta\mu_f\mu_\phi$.

PROOF. See Appendix B.

Remark 4 *It can be easily verified that there exist quadratic functions f, ϕ in the classes specified in the Theorem for which the rate bound $\rho = \eta\mu_f\mu_\phi$ is tight.*

Consider the class of Lyapunov function candidates (B.1) with $\rho = 0$, that is,

$$V = \frac{1}{2} \tilde{z}^T P \tilde{z} + \gamma \int_0^{y_2 - y_2^{\text{opt}}} \psi_2(\tau) d\tau. \quad (20)$$

where $\psi_2(\tau) = \Delta_2(\tau)$ with Δ_2 defined in (15), and P satisfies LMI (19) with a strict inequality. Such Lyapunov functions follow from the Popov criterion, i.e., it is known that when the conditions in the Popov criterion (Lemma 3) hold such a P exists and (20) is a valid Lyapunov function for the Lur'e system (14) (15) (Khalil (2002)). The following proposition establishes a link between the Bregman divergence and the Popov criterion in the context of the MD method.

Proposition 1 (link between Popov criterion and Bregman divergence) *Consider the class of Lyapunov functions in (20) for the MD method (9), which follow from the Popov criterion. These Lyapunov functions include the Bregman divergence function $D_{\bar{\phi}}(z, z^{\text{opt}})$ as a special case.*

PROOF. As the nonlinear function ψ_2 is given by $\psi_2(\tilde{y}_2) = (\nabla \bar{\phi}(\tilde{y}_2 + y_2^{\text{opt}}) - \mu_{\bar{\phi}}(\tilde{y}_2 + y_2^{\text{opt}})) - (\nabla \bar{\phi}(y_2^{\text{opt}}) - \mu_{\bar{\phi}} y_2^{\text{opt}})$, (20) becomes

$$\begin{aligned} V &= \frac{1}{2} \tilde{z}^T P \tilde{z} + \gamma \int_{y_2^{\text{opt}}}^{y_2} (\nabla \bar{\phi}(\tau) - \mu_{\bar{\phi}} \tau) - (\nabla \bar{\phi}(y_2^{\text{opt}}) - \mu_{\bar{\phi}} y_2^{\text{opt}}) d\tau \\ &= \frac{1}{2} \tilde{z}^T P \tilde{z} + \gamma \int_{z^{\text{opt}}}^z (\nabla \bar{\phi}(\tau) - \mu_{\bar{\phi}} \tau) - (\nabla \bar{\phi}(z^{\text{opt}}) - \mu_{\bar{\phi}} z^{\text{opt}}) d\tau \\ &= \frac{1}{2} \tilde{z}^T P \tilde{z} + \gamma D_{\bar{\phi}}(z, z^{\text{opt}}) - \frac{\gamma \mu_{\bar{\phi}}}{2} \|\tilde{z}\|^2. \end{aligned} \quad (21)$$

We note that the LMI (B.2) in Appendix B, which is an expanded version of (19) when $P = pI_d > 0$, $p \in \mathbb{R}$, holds with a strict inequality when $\rho = 0$, $P = \gamma \mu_{\bar{\phi}} I_d$, $q_1 = \eta \gamma$, $q_2 = 2\eta \gamma \mu_f \mu_{\bar{\phi}}$, and $\eta > 0$. This ensures that V with this P is a valid Lyapunov function, as follows from the proof of Theorem 3. In addition, let $\gamma = 1$, then the Lyapunov function (20) for the Popov criterion reduces to the Bregman divergence from the optimal solution, $D_{\bar{\phi}}(z, z^{\text{opt}})$.

Remark 5 *Proposition 1 shows that the Bregman divergence from the optimal solution, which is the Lyapunov function commonly used in the literature for the MD algorithm (Nemirovskij & Yudin (1983), Krichene et al. (2015)), is a special case of Lyapunov functions that follow from the Popov criterion. This establishes an important connection between the Bregman divergence and the Popov criterion, which illustrates the significance of an IQC analysis in the reformulated problem that has been considered. In particular, an IQC analysis allows multiple IQCs to be combined via conic combinations, and can therefore potentially lead to less conservative convergence rate bounds. This becomes relevant in the discrete-time case and the case where projections are additionally included, which are addressed subsequently in this work.*

4 Discrete-time mirror descent method

Having observed the effectiveness of IQCs in continuous time, we now turn our attention to the convergence rate analysis of MD method in discrete time.

4.1 MD algorithm in the form of Lur'e systems

Similar to the continuous-time case, the discrete-time MD algorithm in (8) can be rewritten as the following Lur'e system,

$$z_{k+1} = Az_k + Bu_k, \quad y_k = Cz_k + Du_k \quad (22)$$

where $u_k = \begin{bmatrix} u_k^{(1)} \\ u_k^{(2)} \end{bmatrix}$, $y_k = \begin{bmatrix} y_k^{(1)} \\ y_k^{(2)} \end{bmatrix}$ the system matrices are

$$\begin{bmatrix} A & B \\ C & D \end{bmatrix} = \begin{bmatrix} (1 - \eta \mu_f \mu_{\bar{\phi}}) I_d & -\eta I_d & -\eta \mu_f I_d \\ \mu_{\bar{\phi}} I_d & 0_d & I_d \\ I_d & 0_d & 0_d \end{bmatrix} \quad (23)$$

and the system input is

$$\begin{bmatrix} u_k^{(1)} \\ u_k^{(2)} \end{bmatrix} = \begin{bmatrix} \nabla f(y_k^{(1)}) - \mu_f y_k^{(1)} \\ \nabla \bar{\phi}(y_k^{(2)}) - \mu_{\bar{\phi}} y_k^{(2)} \end{bmatrix}. \quad (24)$$

We denote z^{opt} as the optimal value of z at steady state, with corresponding equilibrium values $y^{\text{opt}} = (y^{(1),\text{opt}}, y^{(2),\text{opt}})$, x^{opt} , and u^{opt} . Defining $\tilde{u}_k = u_k - u^{\text{opt}}$, we have

$$\tilde{u}_k = \Delta \left(\begin{bmatrix} y_k^{(1)} - y^{(1),\text{opt}} \\ y_k^{(2)} - y^{(2),\text{opt}} \end{bmatrix} \right) \quad (25)$$

where the nonlinear operator Δ in (25) is the same as that used for the continuous-time algorithm in (15).

4.2 Convergence rate bounds via IQCs

There is no exact counterpart for the Popov criterion in discrete time, though we could derive LMI conditions for the discrete-time system (23), (25) via related Lyapunov functions (Park et al. (2019)). Similar ones are the discrete-time Jury-Lee criteria (Jury & Lee (1964), Haddad & Bernstein (1994)). Nonetheless, we remark that in discrete time, all IQCs to characterize monotone and bounded nonlinearities are within the set of Zames-Falb-O'Shea IQCs (Carrasco et al. (2016)). Therefore, we can directly apply the class of Zames-Falb-O'Shea IQCs with a state-space representation as in Lessard et al. (2016). We will only adopt a simple type of the Zames-Falb-O'Shea IQC here, as this is sufficient to obtain a tight convergence rate for the unconstrained MD method.

Lemma 4 (Lessard et al. (2016)) *Suppose $f \in S(\mu_f, L_f)$, x^{opt} is a reference point. The nonlinearity $\nabla f(x) - \nabla f(x^{\text{opt}})$ satisfies the weighted off-by-one IQC defined by $\Pi_{w,f}(j\omega)$ given by*

$$\Pi_{w,f} = \Psi_{w,f}^* M \Psi_{w,f}, \quad M = \begin{bmatrix} 0_d & I_d \\ I_d & 0_d \end{bmatrix}, \quad (26)$$

where $\Psi_{w,f}$ is a transfer function matrix with the following state-space representation,

$$\Psi_{w,f} : \begin{bmatrix} A_{\Psi_{w,f}} & B_{\Psi_{w,f}}^y & B_{\Psi_{w,f}}^u \\ C_{\Psi_{w,f}} & D_{\Psi_{w,f}}^y & D_{\Psi_{w,f}}^u \end{bmatrix} := \begin{bmatrix} 0_d & -KI_d & I_d \\ \bar{\rho}^2 I_d & KI_d & -I_d \\ 0_d & 0_d & I_d \end{bmatrix} \quad (27)$$

where $K = L_f - \mu_f \geq 0$ and $\bar{\rho} \geq 0$.

For $\bar{\phi} \in S(\mu_{\bar{\phi}}, L_{\bar{\phi}})$, we define $\Psi_{w,\bar{\phi}}$ similarly to (27) with matrices $A_{\Psi_{w,\bar{\phi}}}, \dots, D_{\Psi_{w,\bar{\phi}}}^u$.

From Lemma 1, we can obtain that $\nabla f(x) -$

$\nabla f(x^{\text{opt}})$ satisfies the IQC defined by

$$\Pi_{s,f} = \Psi_{s,f}^* M \Psi_{s,f}, \quad M = \begin{bmatrix} 0_d & I_d \\ I_d & 0_d \end{bmatrix} \quad (28)$$

where Ψ_s is a transfer function matrix with the following state-space representation,

$$\Psi_{s,f} : \left[\begin{array}{c|cc} A_{\Psi_{s,f}} & B_{\Psi_{s,f}}^y & B_{\Psi_{s,f}}^u \\ \hline C_{\Psi_{s,f}} & D_{\Psi_{s,f}}^y & D_{\Psi_{s,f}}^u \end{array} \right] := \left[\begin{array}{c|cc} 0_d & 0_d & 0_d \\ \hline 0_d & KI_d & -I_d \\ \hline 0_d & 0_d & I_d \end{array} \right]. \quad (29)$$

where $K = L_f - \mu_f \geq 0$. For $\bar{\phi} \in S(\mu_{\bar{\phi}}, L_{\bar{\phi}})$, we define $\Psi_{s,\bar{\phi}}$ similarly to (29) with matrices $A_{\Psi_{s,\bar{\phi}}}, \dots, D_{\Psi_{s,\bar{\phi}}}^u$.

Then, we can characterize upper bounds on the convergence rate for the discrete-time MD algorithm by applying the discrete-time IQC theorem with the IQC constructed from the conic combination of a sector and a weighted off-by-one IQC for both nonlinearities in (25). A sequence $\{x(k)\}$ converges to x^{opt} linearly with rate $\rho \in (0, 1)$ if there exists $c > 0$ such that $\|x(k) - x^{\text{opt}}\| \leq c\rho^k \|x(0) - x^{\text{opt}}\|$, for all $k \in \mathbb{N}$.

Theorem 4 *The discrete-time MD algorithm (8) with $f \in S(\mu_f, L_f)$ and $\phi \in S(\mu_\phi, L_\phi)$ converges linearly with rate $\bar{\rho} \leq \rho \leq 1$ if the following LMI is feasible for some $P = P^T > 0$, $\alpha = \text{diag}\{\alpha_1, \dots, \alpha_4\} \geq 0$,*

$$\begin{bmatrix} \hat{A}^T P \hat{A} - \rho^2 P & \hat{A}^T P \hat{B} \\ * & \hat{B}^T P \hat{B} \end{bmatrix} + [\hat{C} \ \hat{D}]^T (\alpha \otimes M) [\hat{C} \ \hat{D}] \leq 0 \quad (30)$$

where

$$\begin{aligned} \hat{A} &= \begin{bmatrix} A & 0_{d \times d} & 0_{d \times d} \\ B_{\Psi_{w,f}}^y C_1 & A_{\Psi_{w,f}} & 0_{d \times d} \\ B_{\Psi_{w,\bar{\phi}}}^y C_2 & 0_{d \times d} & A_{\Psi_{w,\bar{\phi}}} \end{bmatrix}, \\ \hat{B} &= \begin{bmatrix} B_1 & B_2 \\ B_{\Psi_{w,f}}^y D_{11} + B_{\Psi_{w,f}}^u & B_{\Psi_{w,f}}^y D_{12} \\ B_{\Psi_{w,\bar{\phi}}}^y D_{21} & B_{\Psi_{w,\bar{\phi}}}^y D_{22} + B_{\Psi_{w,\bar{\phi}}}^u \end{bmatrix}, \\ \hat{C} &= \begin{bmatrix} D_{\Psi_{s,f}}^y C_1 & 0_{2d \times d} & 0_{2d \times d} \\ D_{\Psi_{w,f}}^y C_1 & C_{\Psi_{w,f}} & 0_{2d \times d} \\ D_{\Psi_{s,\bar{\phi}}}^y C_2 & 0_{2d \times d} & 0_{2d \times d} \\ D_{\Psi_{w,\bar{\phi}}}^y C_2 & 0_{2d \times d} & C_{\Psi_{w,\bar{\phi}}} \end{bmatrix}, \\ \hat{D} &= \begin{bmatrix} D_{\Psi_{s,f}}^y D_{11} + D_{\Psi_{s,f}}^u & D_{\Psi_{s,f}}^y D_{12} \\ D_{\Psi_{w,f}}^y D_{11} + D_{\Psi_{w,f}}^u & D_{\Psi_{w,f}}^y D_{12} \\ D_{\Psi_{s,\bar{\phi}}}^y D_{21} & D_{\Psi_{s,\bar{\phi}}}^y D_{22} + D_{\Psi_{s,\bar{\phi}}}^u \\ D_{\Psi_{w,\bar{\phi}}}^y D_{21} & D_{\Psi_{w,\bar{\phi}}}^y D_{22} + D_{\Psi_{w,\bar{\phi}}}^u \end{bmatrix}, \quad (31) \end{aligned}$$

$B_1, B_2, C_1, C_2, D_{11}, \dots, D_{22}$ are partitions of B, C, D in (23), respectively; The other matrices are given in (27), (29) with $K = L_f - \mu_f$, or $K = L_{\bar{\phi}} - \mu_{\bar{\phi}}$, depending on subscripts $f, \bar{\phi}$, respectively.

The system matrices result from the standard factorization and state-space realization for the IQC condition (3) (Scherer & Weiland (2000), Seiler (2015)). The proof is similar to (Lessard et al. 2016, Theorem 4) and is omitted here. The convergence rate ρ in (30) needs to be treated as a constant such that (30) is an LMI. Then, a bisection search on ρ can be carried out to obtain the optimal convergence rate.

4.3 Stepsize selection

It is well-known that the optimal fixed stepsize for the GD method $x_{k+1} = x_k - \eta \nabla f(x_k)$ is $\eta = \frac{2}{L_f + \mu_f}$, rendering the tight upper bound for the convergence rate $\rho = \frac{\kappa_f - 1}{\kappa_f + 1}$, where $\kappa_f = L_f / \mu_f$ (Nesterov (2003), Ruszczynski (2011), Lessard et al. (2016)). However, the choice of constant stepsizes and the corresponding convergence rates for the MD method have not yet been addressed in the literature. In our numerical studies in section 6 we will use the optimal stepsize when the objective functions f , and the DGF ϕ are quadratic, since in this case the optimal stepsize and the corresponding tight upper bound on the rates can be analytically derived. These are stated in the following proposition.

Proposition 2 *Let $f(x) = \frac{1}{2}x^T Fx + p^T x + r$, and $\phi(x) = \frac{1}{2}x^T \Phi x$, where $p, r \in \mathbb{R}^d$ are constant vectors, F and Φ are any positive definite matrices that satisfy $\mu_f I_d \leq F \leq L_f I_d$, and $\mu_\phi I_d \leq \Phi \leq L_\phi I_d$, respectively. Then, the smallest upper bound on the convergence rate for the MD method (6) is given by $\rho = \frac{\kappa_f \kappa_{\bar{\phi}} - 1}{\kappa_f \kappa_{\bar{\phi}} + 1}$, where $\kappa_f = L_f / \mu_f$, $\kappa_{\bar{\phi}} = L_{\bar{\phi}} / \mu_{\bar{\phi}}$ with $\mu_{\bar{\phi}} = (L_\phi)^{-1}$, and $L_{\bar{\phi}} = (\mu_\phi)^{-1}$ are the condition numbers of $f, \bar{\phi}$, respectively, and this convergence rate is achieved with the stepsize $\eta = \frac{2}{L_f L_{\bar{\phi}} + \mu_f \mu_{\bar{\phi}}}$.*

PROOF. See Appendix C.

We will illustrate via the numerical example in Section 6.2 that for such a choice of η the associated tight convergence rate bound $\rho = \frac{\kappa_f \kappa_{\bar{\phi}} - 1}{\kappa_f \kappa_{\bar{\phi}} + 1}$ for quadratic functions coincides with that obtained from the results in this paper for any nonlinear functions $f \in S(\mu_f, L_f)$, and $\phi \in S(\mu_\phi, L_\phi)$. Also when different stepsizes were tried in our numerical computation of the rate bounds, we found that the smallest rate bound was obtained for this choice of stepsize.

A comparison of the convergence rate bounds obtained from our results and those reported in the literature is also presented in Section 6.2.

5 Projected MD and convergence rate

The study on the projected MD algorithm is more challenging due to the existence of a projection in the dynamics. We will show in this section that the IQC

framework developed in the previous section allows to derive bounds for the convergence rate in this case as well.

5.1 Projected MD algorithm in the form of Lur'e systems

The discrete-time MD algorithm with a convex constraint set \mathcal{X} is given by

$$x_{k+1} = \operatorname{argmin}_{x \in \mathcal{X}} \left\{ \nabla f(x_k)^T x + \frac{1}{\eta} D_\phi(x, x_k) \right\}. \quad (32)$$

As commented in Beck & Teboulle (2003), one of the motivations for the use of the Bregman divergence and the design of the distance function ϕ is to reflect the geometry of the given constraints set \mathcal{X} , so that the constraints can be satisfied without incorporating projections. This is achieved when the function ϕ is chosen such that the following property holds

$$\begin{aligned} \|\nabla \phi(x_k)\| &\rightarrow +\infty \text{ as } k \rightarrow \infty, \\ \text{for all sequences } \{x_k \in \operatorname{int} \mathcal{X} : k = 1, 2, \dots\} \quad (33) \\ \text{where } x_k &\rightarrow x \in \operatorname{bd} \mathcal{X} \text{ as } k \rightarrow \infty. \end{aligned}$$

where $\operatorname{bd} \mathcal{X}$ denotes the boundary of \mathcal{X} and $\operatorname{int} \mathcal{X}$ represents the interior of \mathcal{X} . However, when we use a function ϕ that does not satisfy assumption (33), a projected variant should be considered, as in (32) (Beck & Teboulle (2003)).

While (6) finds the optimal point by setting the gradient to zero, the optimization of (32) requires satisfying a differential inclusion to achieve optimality ((Ruszczynski 2011, Theorem 3.34)), i.e.,

$$-\nabla \phi(x_{k+1}) + \nabla \phi(x_k) - \eta \nabla f(x_k) \in N_{\mathcal{X}}(x_{k+1}) \quad (34)$$

where $N_{\mathcal{X}}(x_{k+1})$ represents the normal cone of the convex set \mathcal{X} at x_{k+1} . From the strong convexity of ϕ , we have that x_{k+1} is the unique point satisfying the above inclusion (Beck & Teboulle 2003, Proposition 3.2). Then equivalently,

$$\nabla \phi(x_{k+1}) = \nabla \phi(x_k) - \eta \nabla f(x_k) - \nu T(x_{k+1}) \quad (35)$$

where $\nu > 0$ is a positive parameter and $T(x)$ is an element in $N_{\mathcal{X}}(x)$ such that the above equation is satisfied. Again, letting $z_k = \nabla \phi(x_k)$, we have that

$$z_{k+1} = z_k - \eta \nabla f(\nabla \bar{\phi}(z_k)) - \nu T(\nabla \bar{\phi}(z_{k+1})) \quad (36)$$

where $\bar{\phi}$ is defined exactly the same as (7), i.e., without the set constraint.

Notice that there are two terms involving a composition of nonlinear operators on the right hand side of (36), which means that two transformations need to be carried out analogous to those in the previous section. Additionally, the presence of z_{k+1} on the right-hand side

necessitates an extra state to accommodate this algebraic loop. In order to incorporate the points above, the projected MD algorithm (36) is rewritten as

$$z_{k+1} = Az_k + Bu_k, \quad y_k = Cz_k + Du_k \quad (37)$$

with

$$\begin{aligned} &\begin{bmatrix} A & B \\ C & D \end{bmatrix} \\ &= \begin{bmatrix} (1 - \eta \mu_f \mu_{\bar{\phi}}) I_d & -\eta I_d & -\eta \mu_f I_d & -I_d & 0_d \\ \mu_{\bar{\phi}} I_d & 0_d & I_d & 0_d & 0_d \\ I_d & 0_d & 0_d & 0_d & 0_d \\ \mu_{\bar{\phi}} (1 - \eta \mu_f \mu_{\bar{\phi}}) I_d & -\eta \mu_{\bar{\phi}} I_d & -\eta \mu_{\bar{\phi}} \mu_f I_d & -\mu_{\bar{\phi}} I_d & I_d \\ (1 - \eta \mu_f \mu_{\bar{\phi}}) I_d & -\eta I_d & -\eta \mu_f I_d & -I_d & 0_d \end{bmatrix} \end{aligned} \quad (38)$$

and system input

$$u_k = \begin{bmatrix} u_k^{(1)} \\ u_k^{(2)} \\ u_k^{(3)} \\ u_k^{(4)} \end{bmatrix} = \begin{bmatrix} \nabla f(y_k^{(1)}) - \mu_f y_k^{(1)} \\ \nabla \bar{\phi}(y_k^{(2)}) - \mu_{\bar{\phi}} y_k^{(2)} \\ \nu T(y_k^{(3)}) \\ \nabla \bar{\phi}(y_k^{(4)}) - \mu_{\bar{\phi}} y_k^{(4)} \end{bmatrix}. \quad (39)$$

Denote z^{opt} as the optimal value of z at steady state, with corresponding equilibrium values y^{opt} , and u^{opt} . It is worth noting that in this reformulation, $y_k^{(1)} = x_k$, $y_k^{(2)} = z_k$, $y_k^{(3)} = z_{k+1}$ and $y_k^{(4)} = x_{k+1}$. Then, we have $y^{(2), \text{opt}} = y^{(4), \text{opt}}$.

Define $\tilde{u}_k = u_k - u^{\text{opt}}$ and $\tilde{y}_k = y_k - y^{\text{opt}}$. Obviously, the input/output pair $(\tilde{u}_k, \tilde{y}_k)$ of the nonlinearity satisfies the Sector IQC and weighted off-by-one IQC with suitable parameters. In particular, the normal cone of a convex set \mathcal{X} at a point $x \in \mathcal{X}$, is equal to the subdifferential of the indicator function on \mathcal{X} , which is convex (Rockafellar 1997, p. 215). Thus, we have

$$(T(x) - T(y))^T (x - y) \geq 0, \forall x \in \mathcal{X}, \forall y \in \mathcal{X},$$

which is a property that also follows from the definition of the normal cone. Then, $T(x)$ satisfies for all trajectories in \mathcal{X} the Sector and weighted off-by-one IQCs with $m = 0$ and $L = \infty$ (Lessard et al. (2016)). We include the state-space realization for $\Psi_{s,T}$, $\Psi_{w,T}$ as follows,

$$\Psi_{s,T} : \begin{bmatrix} A_{\Psi_{s,T}} & B_{\Psi_{s,T}}^y & B_{\Psi_{s,T}}^u \\ C_{\Psi_{s,T}} & D_{\Psi_{s,T}}^y & D_{\Psi_{s,T}}^u \end{bmatrix} := \begin{bmatrix} 0_d & 0_d & 0_d \\ 0_d & 0_d & I_d \\ 0_d & I_d & 0_d \end{bmatrix},$$

$$\Psi_{w,T} : \left[\begin{array}{c|cc} A_{\Psi_{w,T}} & B_{\Psi_{w,T}}^y & B_{\Psi_{w,T}}^u \\ \hline C_{\Psi_{w,T}} & D_{\Psi_{w,T}}^y & D_{\Psi_{w,T}}^u \end{array} \right] := \left[\begin{array}{c|cc} 0_d & -I_d & 0_d \\ \hline 0_d & 0_d & I_d \\ \hline \bar{\rho}^2 I_d & I_d & 0_d \end{array} \right].$$

The above weighted off-by-one IQC in the frequency domain is given by Boczar et al. (2017).

5.2 Repeated nonlinearities

We observe that there are repeated nonlinearities present in equation (39). To obtain less conservative results, these repeated nonlinearities must be properly addressed. The largest class of bounded convolution multipliers to deal with repeated nonlinearities have been proposed in the literature (Kulkarni & Safonov (2002), D'Amato et al. (2001)). In this paper, we opt for a special class of IQCs described below, which are sufficient for providing feasible solutions with a good convergence rate bound.

Notably, $y_k^{(2)} - y_k^{(4)}$ and $u_k^{(2)} - u_k^{(4)}$, as the input and output of a nonlinearity, also satisfy the Sector IQC in Lemma 1. It is evident that they also satisfy the weighted-off-by-one IQC in Lemma 4. As a result, we obtain two additional IQCs necessary for describing the repeated nonlinearities in (39).

It is worth mentioning that it may be possible to select additional classes of IQCs from Kulkarni & Safonov (2002), D'Amato et al. (2001) in order to achieve less conservative rates. However, exploring these possibilities falls beyond the scope of this paper.

5.3 Convergence rate analysis

Building upon previous discussions, for each nonlinearity in (39), we incorporate one Sector IQC and one weighted off-by-one IQC, yielding $2 \times 4 = 8$ IQCs. Additionally, for repeated nonlinearities, we also use both the Sector and weighted off-by-one IQCs, amounting to $2 \times 1 = 2$ IQCs. Altogether, this results in a conic combination of 10 IQCs to characterize the nonlinearity in (39). A theorem stemming from this discussion, analogous to Theorem 4, can be obtained with its proof omitted for brevity.

Theorem 5 *The mirror descent algorithm converges linearly with rate $\bar{\rho} \leq \rho \leq 1$ if there exists a matrix $P = P^T > 0$, $\alpha = \text{diag}\{\alpha_1, \dots, \alpha_{10}\} \geq 0$ such that the following inequality holds*

$$\begin{bmatrix} \hat{A}^T P \hat{A} - \rho^2 P & \hat{A}^T P \hat{B} \\ * & \hat{B}^T P \hat{B} \end{bmatrix} + [\hat{C} \ \hat{D}]^T (\alpha \otimes M) [\hat{C} \ \hat{D}] \leq 0, \quad (40)$$

where \hat{A} , \hat{B} , \hat{C} , \hat{D} are given in Appendix D.

Similar to Theorem 4, the system matrices are obtained through the standard factorization and state-space realization for the IQC condition (3). To the best of our knowledge, this theorem provides the first systematic method for computing convergence rate bounds for the projected MD method (32) with a constant stepsize. These bounds are further illustrated in the next section via numerical examples.

6 Numerical Examples

In this section, we present four numerical examples to illustrate the IQC analysis for the continuous-time, discrete-time and projected MD algorithm, respectively.

6.1 Continuous-time MD method

We investigate and compare the feasibility of the IQC condition (3) when using merely the Sector IQC defined by (16), and when using the conic combination of the Sector and Popov IQCs defined by (A.1). The frequency-domain condition (3) under (16) can be easily transformed into an LMI via the Kalman–Yakubovich–Popov (KYP) lemma. Condition (3) under (A.1) is satisfied if and only if (19) in Theorem 3 is feasible for some $\rho > 0$. Let $\eta = 1$, $\mu_f = 1$ and $\mu_{\bar{\phi}} = 1$, and $L_f = L_{\bar{\phi}}$. The feasibility of the IQCs (for some $\rho > 0$) with varying composite condition number $\kappa = \frac{L_f}{\mu_f} \cdot \frac{L_{\bar{\phi}}}{\mu_{\bar{\phi}}}$ is shown in Fig. 2. It should be noted that the largest convergence rate bound is $\rho = \eta \mu_f \mu_{\bar{\phi}}$ (Theorem 3) and is obtained with a conic combination of Sector and Popov IQCs. Note that the MD algorithm should converge for any $L_f > \mu_f$ and $L_{\bar{\phi}} > \mu_{\bar{\phi}}$. However, we can observe that the Sector IQC defined by (16) fails to certify the convergence of the MD method for $\kappa \geq 34$. On the other hand, using the conic combination of the Sector and Popov IQCs defined by (A.1) suffices to certify its convergence for arbitrary κ .

Since the Popov IQC corresponds to the Bregman divergence function in time-domain analysis, this example thus highlights the importance of adopting Bregman-like Lyapunov functions in the convergence analysis.

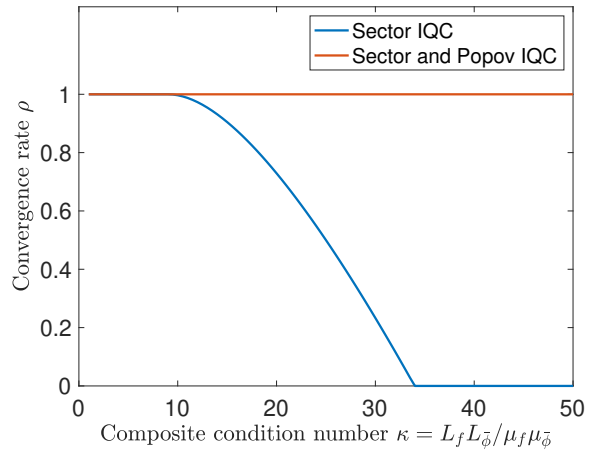


Fig. 2. Convergence rate for the continuous-time MD method as a function of the composite condition number $\kappa = \frac{L_f}{\mu_f} \cdot \frac{L_{\bar{\phi}}}{\mu_{\bar{\phi}}}$, derived from the Sector IQC (16) and Sector and Popov IQC (A.1), respectively. The MD method parameters have been set as $\eta = \mu_f = \mu_{\bar{\phi}} = 1$. Note that the largest convergence rate bound is $\rho = \eta \mu_f \mu_{\bar{\phi}} = 1$, as established in Theorem 3, and we let $\rho = 0$ when the associated LMI is infeasible.

6.2 Discrete-time MD method

Next, we present the convergence rate for the discrete-time MD method. Let $\mu_f = 1$, $\mu_{\bar{\phi}} = 1$, and $L_f = L_{\bar{\phi}}$. Let the stepsize be $\eta = \frac{2}{L_f L_{\bar{\phi}} + \mu_f \mu_{\bar{\phi}}}$ as Section 4.3 suggested. We compare the smallest convergence rate obtained from (30) in Theorem 4 with that obtained from the semidefinite programs (SDPs) in Sun et al. (2022), where the stepsize and convergence rate are both decision variables. The SDPs in Sun et al. (2022) are derived from the Lyapunov function $V(z_k) = \rho^{-k} D_{\bar{\phi}}(z_k, z^{\text{opt}})$, which is the Bregman divergence function when $\rho = 1$. The relation between the composite condition number $\kappa = \frac{L_f}{\mu_f} \cdot \frac{L_{\bar{\phi}}}{\mu_{\bar{\phi}}}$ and the convergence rate ρ is shown in Fig. 3. We can observe that using the IQC analysis provides a tighter bound for the convergence rate. We remark that the convergence rate bound obtained in this example using the IQC analysis coincides with the curve $\rho = \frac{\kappa-1}{\kappa+1}$. This illustrates that this bound is also tight since Proposition 2 shows that this expression is the smallest upper bound on the convergence rate for all quadratic functions $f \in S(\mu_f, L_f)$ and $\bar{\phi} \in S(\mu_{\bar{\phi}}, L_{\bar{\phi}})$.

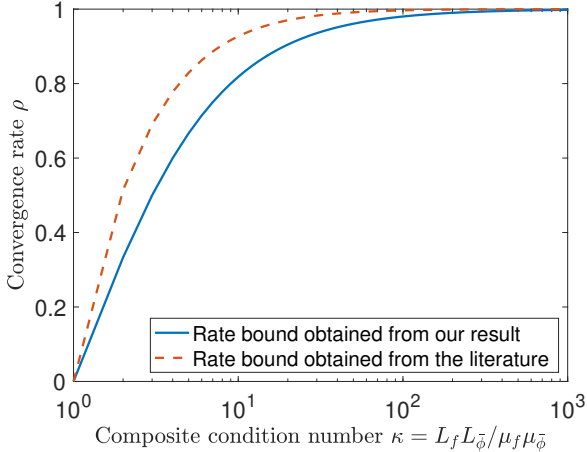


Fig. 3. Convergence rate obtained from (30) in Theorem 4 and from the SDPs in Sun et al. (2022). The convergence rate bound obtained from our result coincides with the curve $\rho = \frac{\kappa-1}{\kappa+1}$.

6.3 Convergence rate with quadratic functions

When comparing the convergence rate bounds between the GD and MD algorithms, we have $\frac{\kappa_f-1}{\kappa_f+1} \leq \frac{\kappa-1}{\kappa+1}$. This is due to $\kappa = \kappa_f \kappa_{\bar{\phi}} \geq \kappa_f$. Hence, the distance generating function ϕ used in the MD method does not necessarily result in a faster convergence rate than the GD method under constant stepsizes. The potential for improvement in the convergence rate of the MD algorithm is dependent on the specific structure of the distance generating function ϕ , which must be carefully tailored to the function f .

To illustrate this, we present a simple example that

compares the convergence rate of the GD and MD methods when applied to a quadratic convex objective function. Specifically, we consider the following optimization problem

$$\min_{x \in \mathbb{R}^2} \left\{ f(x) := \frac{1}{2} x^T F x + p^T x \right\}$$

where

$$F = \begin{bmatrix} 100 & -1 \\ -1 & 1 \end{bmatrix}, \quad p = \begin{bmatrix} 1 \\ 10 \end{bmatrix}.$$

The optimal solution and value can be easily obtained,

$$x^{\text{opt}} = -F^{-1}p = \begin{bmatrix} -0.1111 \\ -10.1111 \end{bmatrix}, \quad f^{\text{opt}} = -50.6111.$$

It is clear that $f \in S(\mu_f, L_f)$ with $\mu_f = 0.9899$ and $L_f = 100.0101$. Next, we select DGF $\bar{\phi}(x) = \frac{1}{2} x^T \bar{\Phi} x$,

where $\bar{\Phi} = \begin{bmatrix} 10 & 1 \\ 1 & 1 \end{bmatrix}$. As a result, its convex conjugate

is $\bar{\phi}(z) = \frac{1}{2} z^T \bar{\Phi} z$, and $\bar{\phi}(z) \in S(\mu_{\bar{\phi}}, L_{\bar{\phi}})$, where $\mu_{\bar{\phi}} = 0.09891$ and $L_{\bar{\phi}} = 1.1233$. The convergence rate bound of the GD algorithm is $\rho_g = \frac{L_f/\mu_f-1}{L_f/\mu_f+1} = 0.9804$, while the convergence rate bound of the MD algorithm given by Proposition 2 (which holds for arbitrary quadratic functions in the specified classes) is

$$\rho = \frac{L_f L_{\bar{\phi}} / \mu_f \mu_{\bar{\phi}} - 1}{L_f L_{\bar{\phi}} / \mu_f \mu_{\bar{\phi}} + 1} = 0.9982 > \rho_g.$$

Interestingly, due to the specific structures of F and $\bar{\Phi}$, the spectrum for $F\bar{\Phi}$ in (C.2) becomes $0.9576 \leq \lambda \leq 11.4868$. As such, a more precise convergence rate bound is

$$\rho_m = \frac{11.4868/0.9576 - 1}{11.4868/0.9576 + 1} = 0.8461 < \rho_g,$$

indicating an accelerated convergence compared to the GD method. This observation is supported by the optimization errors $|f(x_k) - f^{\text{opt}}|$ for both the GD and MD methods, depicted in Fig. 4. Applying the MD method here can be viewed as a form of the preconditioning gradient descent (Maddison et al. (2021)). For more general objective functions, investigating the potential for accelerated convergence rates using the MD method will be an interesting extension for future research.

6.4 Projected MD method

Lastly, we present the convergence rate of the projected MD algorithm. Let $L_f = L_{\bar{\phi}} = 1$ and $\mu_f = \mu_{\bar{\phi}}$. We demonstrate the relation between the composite condition number $\kappa = \frac{L_f}{\mu_f} \cdot \frac{L_{\bar{\phi}}}{\mu_{\bar{\phi}}}$ and convergence rate ρ using Theorem 5. For the stepsize selection, we start by

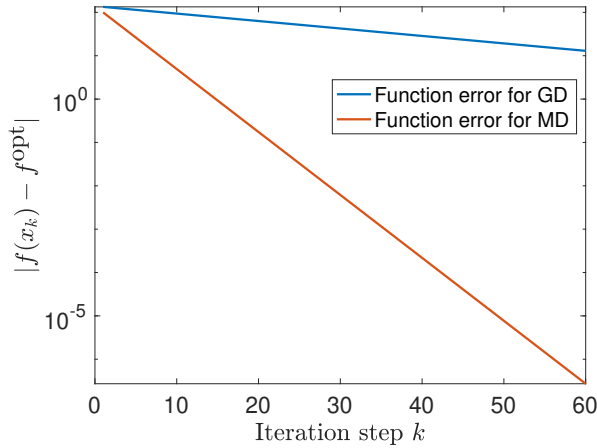


Fig. 4. Optimization errors for GD and MD methods, respectively.

looking for the closest stepsize to $\eta = \frac{2}{L_f L_{\tilde{\phi}} + \mu_f \mu_{\tilde{\phi}}}$ for which the LMIs are feasible, through a bisection search with fixed $\rho = 1$. After finding a suitable stepsize, we then use the bisection method again to search for smallest rate bound. The result is depicted in Fig. 5, showing the smallest rate bounds we can obtain from the proposed IQCs, after a search over different stepsizes was also carried out. It is important to note that the conver-

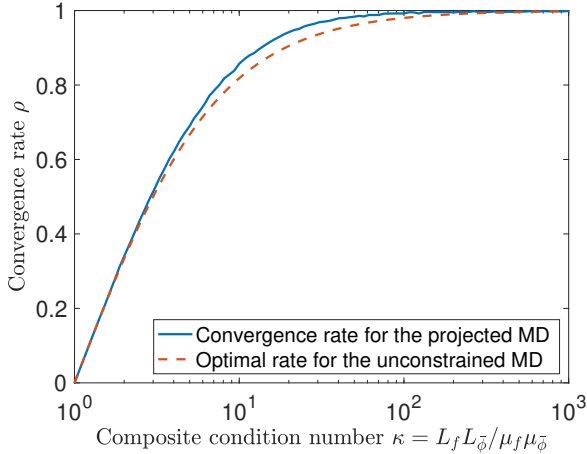


Fig. 5. Convergence rate for the projected MD algorithm (32) obtained from Theorem 5.

gence rate we obtain in this case is slightly larger than the one in the unconstrained scenario. This is due to the presence of additional nonlinear term $\nu T(x_{k+1})$ in (36) and the repeated nonlinearities in (39). As a direction for future work, it would be intriguing to investigate the possibility of obtaining a tighter convergence rate bound by employing more advanced IQCs.

7 Conclusion

An integral quadratic constraint analysis framework has been established for the mirror descent method

in both continuous-time and discrete-time settings. In the continuous-time setting, we demonstrated that the Bregman divergence function is a special case of the Lyapunov functions associated with the Popov criterion when these are applied to an appropriate reformulation of the MD dynamics. In the discrete-time setting, we established upper bounds for the convergence rate via appropriate IQCs applied to the transformed system. It has also been illustrated via numerical examples that the convergence rate bound for the unconstrained case is tight. Future endeavors include extending the framework developed to other related algorithms such as accelerated MD methods.

Acknowledgements

This work was partly supported by ERC starting grant 679774, and the Japanese Ministry of the Environment. M. Li is also supported by Japan Society for the Promotion of Science (JSPS) KAKENHI under Grant 24K23864. For the purpose of open access, the authors have applied a Creative Commons Attribution (CC BY) licence to any Author Accepted Manuscript version arising.

References

- Beck, A. & Teboulle, M. (2003), ‘Mirror descent and non-linear projected subgradient methods for convex optimization’, *Operations Research Letters* **31**(3), 167–175.
- Boczar, R., Lessard, L., Packard, A. & Recht, B. (2017), ‘Exponential stability analysis via integral quadratic constraints’, *arXiv preprint arXiv:1706.01337*.
- Borovykh, A., Kantas, N., Parpas, P. & Pavliotis, G. A. (2022), ‘Stochastic mirror descent for convex optimization with consensus constraints’, *arXiv preprint arXiv:2201.08642*.
- Bregman, L. M. (1967), ‘The relaxation method of finding the common point of convex sets and its application to the solution of problems in convex programming’, *USSR computational mathematics and mathematical physics* **7**(3), 200–217.
- Bubeck, S. et al. (2015), ‘Convex optimization: Algorithms and complexity’, *Foundations and Trends® in Machine Learning* **8**(3-4), 231–357.
- Carrasco, J., Heath, W. P. & Lanzon, A. (2013), ‘Equivalence between classes of multipliers for slope-restricted nonlinearities’, *Automatica* **49**(6), 1732–1740.
- Carrasco, J., Turner, M. C. & Heath, W. P. (2016), ‘Zames–Falb multipliers for absolute stability: From O’shea’s contribution to convex searches’, *European Journal of Control* **28**, 1–19.
- D’Amato, F. J., Rotea, M. A., Megretski, A. & Jönsson, U. (2001), ‘New results for analysis of systems with repeated nonlinearities’, *Automatica* **37**(5), 739–747.
- De Persis, C. & Monshizadeh, N. (2017), ‘Bregman storage functions for microgrid control’, *IEEE Transactions on Automatic Control* **63**(1), 53–68.
- Dhingra, N. K., Khong, S. Z. & Jovanović, M. R. (2018), ‘The proximal augmented lagrangian method for non-

- smooth composite optimization', *IEEE Transactions on Automatic Control* **64**(7), 2861–2868.
- Doan, T. T., Bose, S., Nguyen, D. H. & Beck, C. L. (2018), 'Convergence of the iterates in mirror descent methods', *IEEE control systems letters* **3**(1), 114–119.
- Duchi, J. C., Agarwal, A., Johansson, M. & Jordan, M. I. (2012), 'Ergodic mirror descent', *SIAM Journal on Optimization* **22**(4), 1549–1578.
- Haddad, W. M. & Bernstein, D. S. (1994), 'Parameter-dependent lyapunov functions and the discrete-time popov criterion for robust analysis', *Automatica* **30**(6), 1015–1021.
- Hu, B. & Seiler, P. (2016), 'Exponential decay rate conditions for uncertain linear systems using integral quadratic constraints', *IEEE Transactions on Automatic Control* **61**(11), 3631–3637.
- Jayawardhana, B., Ortega, R., Garcia-Canseco, E. & Castanos, F. (2007), 'Passivity of nonlinear incremental systems: Application to PI stabilization of nonlinear rlc circuits', *Systems & control letters* **56**(9–10), 618–622.
- Jönsson, U. (1997), 'Stability analysis with Popov multipliers and integral quadratic constraints', *Systems & Control Letters* **31**(2), 85–92.
- Jönsson, U. (2001), 'Lecture notes on integral quadratic constraints', <https://people.kth.se/~uj/5B5744/Lecturenotes.ps>.
- Juditsky, A., Kwon, J. & Moulines, É. (2022), 'Unifying mirror descent and dual averaging', *Mathematical Programming* pp. 1–38.
- Jury, E. & Lee, B. (1964), 'On the stability of a certain class of nonlinear sampled-data systems', *IEEE Transactions on Automatic Control* **9**(1), 51–61.
- Khalil, H. K. (2002), 'Nonlinear systems', *Prentice-Hall, New Jersey*.
- Krichene, W., Bayen, A. & Bartlett, P. (2015), 'Accelerated mirror descent in continuous and discrete time', *Advances in neural information processing systems* **28**, 2845–2853.
- Kulkarni, V. V. & Safonov, M. G. (2002), 'All multipliers for repeated monotone nonlinearities', *IEEE Transactions on Automatic Control* **47**(7), 1209–1212.
- Lessard, L., Recht, B. & Packard, A. (2016), 'Analysis and design of optimization algorithms via integral quadratic constraints', *SIAM Journal on Optimization* **26**(1), 57–95.
- Li, M., Chesi, G. & Hong, Y. (2020), 'Input-feedforward-passivity-based distributed optimization over jointly connected balanced digraphs', *IEEE Transactions on Automatic Control*.
- Li, M., Laib, K. & Lestas, I. (2022), 'Convergence rate bounds for the mirror descent method: IQCs and the bregman divergence', in '2022 IEEE 61st Conference on Decision and Control (CDC)', IEEE, pp. 6326–6331.
- Lu, H., Freund, R. M. & Nesterov, Y. (2018), 'Relatively smooth convex optimization by first-order methods, and applications', *SIAM Journal on Optimization* **28**(1), 333–354.
- Maddison, C. J., Paulin, D., Teh, Y. W. & Doucet, A. (2021), 'Dual space preconditioning for gradient descent', *SIAM Journal on Optimization* **31**(1), 991–1016.
- Megretski, A. & Rantzer, A. (1997), 'System analysis via integral quadratic constraints', *IEEE Transactions on Automatic Control* **42**(6), 819–830.
- Mertikopoulos, P., Lecuat, B., Zenati, H., Foo, C.-S., Chandrasekhar, V. & Piliouras, G. (2018), 'Optimistic mirror descent in saddle-point problems: Going the extra (gradient) mile', in 'International Conference on Learning Representations'.
- Monshizadeh, N. & Lestas, I. (2019), 'Secant and Popov-like conditions in power network stability', *Automatica* **101**, 258–268.
- Moore, J. & Anderson, B. (1968), 'A generalization of the Popov criterion', *Journal of the Franklin Institute* **285**(6), 488–492.
- Nedic, A. & Lee, S. (2014), 'On stochastic subgradient mirror-descent algorithm with weighted averaging', *SIAM Journal on Optimization* **24**(1), 84–107.
- Nemirovskij, A. S. & Yudin, D. B. (1983), *Problem complexity and method efficiency in optimization*, Wiley-Interscience.
- Nesterov, Y. (2003), *Introductory lectures on convex optimization: A basic course*, Vol. 87, Springer Science & Business Media.
- Park, J., Lee, S. Y. & Park, P. (2019), 'A less conservative stability criterion for discrete-time lur'e systems with sector and slope restrictions', *IEEE Transactions on Automatic Control* **64**(10), 4391–4395.
- Rantzer, A. (1996), 'On the Kalman–Yakubovich–Popov lemma', *Systems & Control Letters* **28**(1), 7–10.
- Raskutti, G. & Mukherjee, S. (2015), 'The information geometry of mirror descent', *IEEE Transactions on Information Theory* **61**(3), 1451–1457.
- Rockafellar, R. T. (1997), *Convex Analysis*, Vol. 18, Princeton University Press.
- Rockafellar, R. T. & Wets, R. J.-B. (2009), *Variational analysis*, Vol. 317, Springer Science & Business Media.
- Ruszczynski, A. (2011), *Nonlinear Optimization*, Princeton University Press.
- Scherer, C. W., Ebenbauer, C. & Holicki, T. (2023), 'Optimization algorithm synthesis based on integral quadratic constraints: A tutorial', in '2023 62nd IEEE Conference on Decision and Control (CDC)', IEEE, pp. 2995–3002.
- Scherer, C. & Weiland, S. (2000), 'Linear matrix inequalities in control', *Lecture Notes, Dutch Institute for Systems and Control, Delft, The Netherlands* **3**(2).
- Seiler, P. (2015), 'Stability analysis with dissipation inequalities and integral quadratic constraints', *IEEE Transactions on Automatic Control* **60**(6), 1704–1709.
- Simpson-Porco, J. W. (2018), 'A Hill-Moylan lemma for equilibrium-independent dissipativity', in '2018 Annual American Control Conference (ACC)', IEEE, pp. 6043–6048.

Sun, Y., Fazlyab, M. & Shahrampour, S. (2022), ‘On centralized and distributed mirror descent: Convergence analysis using quadratic constraints’, *IEEE Transactions on Automatic Control*.

Wibisono, A., Wilson, A. C. & Jordan, M. I. (2016), ‘A variational perspective on accelerated methods in optimization’, *proceedings of the National Academy of Sciences* **113**(47), E7351–E7358.

Yuan, D., Hong, Y., Ho, D. W. & Jiang, G. (2018), ‘Optimal distributed stochastic mirror descent for strongly convex optimization’, *Automatica* **90**, 196–203.

Appendix

A Proof of Theorem 2

We prove this theorem by applying the extension of Theorem 1 in (Jönsson 1997, Theorem 1) that allows the consideration of conic combinations of IQCs with essentially bounded multipliers $\Pi(j\omega)$, with the Popov IQC. The closed-loop system with $\tau\Delta$ is well-posed since the system we are investigating is the MD algorithm with τ interpreted as a scaling of the gradients. Then, the first condition of Theorem 1 is satisfied. We use a conic combination the Sector and Popov IQCs defined by Π and $\Pi_P(j\omega)$ given by (16) and (17), respectively. In particular, $\Delta \in \text{IQC}(\Pi)$, where $\Pi(j\omega)$ takes the form

$$\begin{aligned} \Pi(j\omega) &= \begin{bmatrix} 0_d & 0_d & (\alpha_1(L_f - \mu_f) - \beta_1 j\omega)I_d & 0_d \\ 0_d & 0_d & 0_d & (\alpha_2(L_{\bar{\phi}} - \mu_{\bar{\phi}}) - \beta_2 j\omega)I_d \\ * & * & -2\alpha_1 I_d & 0_d \\ * & * & 0_d & -2\alpha_2 I_d \end{bmatrix} \\ &:= \begin{bmatrix} \Pi_{11}(j\omega) & \Pi_{12}(j\omega) \\ \Pi_{12}^*(j\omega) & \Pi_{22}(j\omega) \end{bmatrix}. \end{aligned} \quad (\text{A.1})$$

Since $\Pi_{11}(j\omega) \geq 0$ and $\Pi_{22}(j\omega) \leq 0$, the second condition of Theorem 1 is satisfied. Condition (3) in Theorem 1 is satisfied if

$$\begin{aligned} & -\beta_1^2 \omega^4 + (-\eta^2 \beta_2^2 + 2\alpha_1 \eta(L_f + \mu_f)\beta_2 \\ & + 4\alpha_1 \alpha_2 - \alpha_1^2(L_f - \mu_f)^2 + 2\alpha_2 \beta_1 \eta L_{\bar{\phi}} + 2\alpha_2 \beta_1 \eta \mu_{\bar{\phi}}) \omega^2 \\ & + \eta^2 (4\alpha_1 \alpha_2 L_f \mu_f L_{\bar{\phi}} \mu_{\bar{\phi}} - \alpha_2^2(L_{\bar{\phi}} - \mu_{\bar{\phi}})^2) > 0, \quad \forall \omega \in \mathbb{R}. \end{aligned} \quad (\text{A.2})$$

Clearly, a necessary condition for the above inequality to hold is $\beta_1 = 0$, which also coincides with the multiplier condition in Jönsson (1997). To show that it is feasible, we let $\alpha_2 = 1$, α_1, β_2 take the values of $\alpha_1^* = \frac{(L_{\bar{\phi}} - \mu_{\bar{\phi}})^2}{4L_f L_{\bar{\phi}} \mu_f \mu_{\bar{\phi}}}$,

and $\beta_2^* = \frac{\alpha_1^*(L_f + \mu_f) + 2\sqrt{\alpha_1^{*2} L_f \mu_f + \alpha_1^*}}{\eta}$, respectively, and the left hand side of (A.2) becomes zero. Then, there exist $0 < \beta_2 < \beta_2^*$ and $\alpha_1 > \alpha_1^*$ such that (A.2) is satisfied for all $\omega \in \mathbb{R}$. The stability implies $v \in \mathbf{L}_2[0, \infty)$ for $e, g \in \mathbf{L}_2[0, \infty)$ in (2). For the error system (14), the initial condition response of $z_0 - z^{\text{opt}}$ can be represented by the external input $g = Ce^{At}(z_0 - z^{\text{opt}})$, which satisfies $g \in \mathbf{L}_2[0, \infty)$ and $g \rightarrow 0$ as $t \rightarrow \infty$. This means that $v \rightarrow 0$ as $t \rightarrow \infty$ according to (Megretski & Rantzer 1997, Proposition 1), and the system trajectories converge to zero. Thus, the trajectory of $x = \nabla \bar{\phi}(z)$ for any

input z_0 converges to the optimal solution of problem (4).

B Proof of Theorem 3

Consider in (14), (15) the transformation $\tilde{z}_\rho(t) := e^{\rho t} z(t)$, the modified transfer function $G_\rho(s) := C(sI - A - \rho I)^{-1}B + D$ with (A, B, C, D) given in (13), and $\Delta_\rho(t, v(t)) := e^{\rho t} \Delta(e^{-\rho t} v(t))$ with Δ given in (15). Note that $G_\rho(s)$ is the transfer function of the system with input $\tilde{u}_\rho(t) := e^{\rho t} \tilde{u}(t)$, output $\tilde{y}_\rho(t) := e^{\rho t} \tilde{y}(t)$, and state vector $\tilde{z}_\rho(t)$.

According to Hu & Seiler (2016), the closed-loop system of $G(s)$ and Δ in (14), (15) is exponentially stable with rate ρ iff the closed-loop system of $G_\rho(s)$ and Δ_ρ is linearly stable, i.e., $\|\tilde{z}_\rho(t)\| \leq c\|\tilde{z}_\rho(0)\|$, $\forall t \geq 0$, for some $c > 0$.

In the remainder of the proof we show via a Lyapunov function that this linear stability property holds when the LMI (19) holds. Consider the following Lyapunov-like function for the transformed system

$$V_\rho = \frac{1}{2} \tilde{z}_\rho^T P \tilde{z}_\rho + \gamma \int_0^t e^{\rho \tau} \Delta_2(e^{-\rho \tau} \tilde{y}_\rho^{(2)}(\tau))^T \dot{\tilde{y}}_\rho^{(2)}(\tau) d\tau \quad (\text{B.1})$$

where $P = P^T > 0$ satisfying (19).

The integral term can be rewritten as the line integral $\gamma \int_0^{\tilde{y}_\rho^{(2)}(t)} \Delta_\rho^{(2)}(\tau, \tilde{y}_\rho(\tau)) d\tilde{y}_\rho^{(2)}(\tau)$. As $\Delta_\rho^{(2)}$ is slope-restricted with respect to $\tilde{y}_\rho^{(2)}(t)$ on sector $[0, L_{\bar{\phi}} - \mu_{\bar{\phi}}]$, it follows that

$$\begin{aligned} 0 &\leq \gamma \int_0^{\tilde{y}_\rho^{(2)}(t)} \Delta_\rho^{(2)}(\tau, \tilde{y}_\rho(\tau)) d\tilde{y}_\rho^{(2)}(\tau) \\ &\leq \frac{\gamma (L_{\bar{\phi}} - \mu_{\bar{\phi}})}{2} \|\tilde{y}_\rho^{(2)}(t)\|^2. \end{aligned}$$

Moreover, due to the structure of D in (11), $(I - D\Delta_\rho)$ is invertible with the inverse having a bounded gain, hence $(I - D\Delta_\rho)\tilde{y}_\rho = C\tilde{z}_\rho$ implies $\|\tilde{y}_\rho\| \leq \|(I - D\Delta_\rho)^{-1}C\| \cdot \|\tilde{z}_\rho\|$. Thus, we have the following linear bounds on V_ρ w.r.t. the Euclidean norm of the state vector \tilde{z}_ρ , $\alpha_1 \|\tilde{z}_\rho\|^2 \leq V_\rho \leq \alpha_2 \|\tilde{z}_\rho\|^2$ for some $\alpha_1, \alpha_2 > 0$. We also have

$$\begin{aligned} \dot{V}_\rho &= \tilde{z}_\rho^T P (\tilde{A}_\rho \tilde{z}_\rho - \tilde{B} \tilde{u}_\rho) + (\Delta_\rho(t, \tilde{y}_\rho))^T \Gamma C (\tilde{A}_\rho \tilde{z}_\rho - \tilde{B} \tilde{u}_\rho) \\ &= \frac{1}{2} \begin{bmatrix} \tilde{z}_\rho \\ -\tilde{u}_\rho \end{bmatrix}^T \begin{bmatrix} P \tilde{A}_\rho + \tilde{A}_\rho^T P & P \tilde{B} - \tilde{C}_\rho^T \\ * & -(\tilde{D} + \tilde{D}^T) \end{bmatrix} \begin{bmatrix} \tilde{z}_\rho \\ -\tilde{u}_\rho \end{bmatrix} \\ &\quad - \tilde{z}_\rho^T \tilde{C}_\rho^T \tilde{u}_\rho + \tilde{u}_\rho^T \tilde{D} \tilde{u}_\rho + \tilde{u}_\rho^T \Gamma C (\tilde{A}_\rho \tilde{z}_\rho - \tilde{B} \tilde{u}_\rho) \\ &\leq -\tilde{u}_\rho^T ((QC + \rho \Gamma C) \tilde{z}_\rho - QD \tilde{u}_\rho + QK^{-1} \tilde{u}_\rho) \\ &= -\tilde{u}_\rho^T Q (\tilde{y}_\rho - K^{-1} \tilde{u}_\rho) - \rho \tilde{u}_\rho^T \Gamma C \tilde{z}_\rho \\ &= -\tilde{u}_\rho^T Q (\tilde{y}_\rho - K^{-1} \tilde{u}_\rho) - \rho \tilde{u}_\rho^T \Gamma (\tilde{y}_\rho - D \tilde{u}_\rho) \\ &\leq 0 \end{aligned}$$

where $\tilde{u}_\rho = \Delta_\rho(t, \tilde{y}_\rho) = e^{\rho t} \Delta(\tilde{y}_\rho e^{-\rho t})$ is the input of $G_\rho(s)$, the first equality follows from $\Gamma C = \begin{bmatrix} 0_d \\ \gamma I_d \end{bmatrix}$, the first inequality follows from (19), and the last inequality follows from the sector-bounded property of each $\Delta_\rho^{(i)}$ (Lemma 1) and $\Gamma D = 0$. Then, $\|\tilde{z}_\rho(t)\|^2 \leq \alpha_1^{-1} V_\rho(t) \leq \alpha^{-1} V_\rho(0) \leq \alpha_1^{-1} \alpha_2 \|\tilde{z}_\rho(0)\|^2$. Therefore, the interconnection of G_ρ and Δ_ρ is linearly stable. As a result, we have $\|z - z^{\text{opt}}\| \leq e^{-\rho t} c \|z_0 - z^{\text{opt}}\|$, for some $c > 0$. Since $z = \nabla \phi(x)$ and $\phi \in S(\mu_\phi, L_\phi)$, we can obtain $\|x - x^{\text{opt}}\| \leq c \frac{L_\phi}{\mu_\phi} e^{-\rho t} \|x_0 - x^{\text{opt}}\|$, indicating that the variable x also converges exponentially with rate ρ . Next, to obtain the largest lower bound on the convergence rate, let us select $P = pI_d > 0$, $p \in \mathbb{R}$ and expand (19) to obtain

$$\begin{bmatrix} 2(\rho - \eta\mu_f\mu_{\bar{\phi}})p & * & \eta\mu_f p - q_2 - 2\rho\gamma + \eta\gamma\mu_f\mu_{\bar{\phi}} \\ \eta p - q_1\mu_{\bar{\phi}} & -\frac{2q_1}{k_1} & * \\ * & q_1 - \eta\gamma & -2\left(\frac{q_2}{k_2} + \eta\gamma\mu_f\right) \end{bmatrix} \leq 0. \quad (\text{B.2})$$

It can be verified that the above LMI always holds when $\rho = \eta\mu_f\mu_{\bar{\phi}}$, $p = \gamma\mu_{\bar{\phi}}$, $q_1 = \eta\gamma$, $q_2 = 0$ and $\gamma > 0$. Note that such ρ is also a tight lower bound on the convergence rate, since it is the largest lower bound on the convergence rate in continuous time for any quadratic functions $f \in S(\mu_f, L_f)$ and $\bar{\phi} \in S(\mu_{\bar{\phi}}, L_{\bar{\phi}})$, i.e., one can construct quadratic functions $f, \bar{\phi}$ in these classes that achieve this rate bound, e.g., quadratic functions $f, \bar{\phi}$ as in Proposition 2 with $F = \mu_f I_d$, $\Phi = L_{\bar{\phi}} I_d$.

Remark 6 We would like to note that there is a direct link between the Popov criterion (Lemma 3) and the LMI (19) in Theorem 3. Firstly, it follows from Hu & Seiler (2016) that Δ_ρ used in the proof Theorem 3 satisfies the Sector IQC in (16), and the following modified Popov IQC

$$\Pi_{P,\rho}(j\omega) = \begin{bmatrix} 0_d & (\rho - j\omega)I_d \\ (\rho + j\omega)I_d & 0_d \end{bmatrix}.$$

It can be established from the proof of Theorem 1 that the closed-loop system of $G_\rho(s)$ and Δ_ρ is stable if

$$\{QK^{-1} - (Q + \rho\Gamma + j\omega\Gamma)G_\rho(j\omega)\}_{\text{H}} \geq \delta I, \quad \forall \omega \in \mathbb{R} \quad (\text{B.3})$$

for some $\delta > 0$. Using the KYP lemma (Rantzer (1996)), we have $\{QK^{-1} - \frac{\delta}{2}I - (Q + \rho\Gamma + j\omega\Gamma)G_\rho(j\omega)\}_{\text{H}} \geq 0$ if and only if

$$\begin{bmatrix} P\tilde{A}_\rho + \tilde{A}_\rho^T P & P\tilde{B} - \tilde{C}_\rho^T \\ * & -(\tilde{D} + \tilde{D}^T) - \delta I \end{bmatrix} \leq 0. \quad (\text{B.4})$$

where $\tilde{A}_\rho = A + \rho I$, $\tilde{B} = -B$, $\tilde{C}_\rho = (Q + 2\rho\Gamma)C + \Gamma C A$, and $\tilde{D} = -QD + QK^{-1} - \Gamma C B$. Note that (B.3) reduces to the condition in Lemma 3 when $\rho = 0$. It should be noted that in (19) we have $\delta = 0$ since linear stability of the interconnection of $G_\rho(s)$ and Δ_ρ is sufficient for the proof of Theorem 3.

C Proof of Proposition 2

The conjugate function of ϕ can be readily derived: $\bar{\phi}(z) = \frac{1}{2}z^T \bar{\Phi} z$, where $\bar{\Phi} = \Phi^{-1}$. Thus, $\mu_{\bar{\phi}} I_d \leq \bar{\Phi} \leq L_{\bar{\phi}} I_d$. Following (8), the discrete-time MD algorithm is written as

$$z_{k+1} = z_k - \eta F \bar{\Phi} z_k - \eta p$$

The error dynamics with respect to the optimal solution z^{opt} is

$$\tilde{z}_{k+1} = \tilde{z}_k - \eta F \bar{\Phi} \tilde{z}_k = (I_d - \eta F \bar{\Phi}) \tilde{z}_k. \quad (\text{C.1})$$

Note that $F \bar{\Phi} = F^{1/2} (F^{1/2} \bar{\Phi} F^{1/2}) F^{-1/2}$, where $F^{1/2}$ is the square root of F , meaning that $F \bar{\Phi}$ is similar to the positive definite matrix $F^{1/2} \bar{\Phi} F^{1/2}$ and thus all its eigenvalues are real and positive. Let λ be an eigenvalue of $F^{1/2} \bar{\Phi} F^{1/2}$ associated with eigenvector x . Then, we have $x^T F^{1/2} \bar{\Phi} F^{1/2} x = \lambda x^T x$. Let $q = F^{1/2} x$, it follows that

$$q^T \bar{\Phi} q = \lambda q^T F^{-1} q.$$

We know that $\mu_{\bar{\phi}} \|q\|^2 \leq q^T \bar{\Phi} q \leq L_{\bar{\phi}} \|q\|^2$, and $1/L_f \|q\|^2 \leq q^T F^{-1} q \leq 1/m_f \|q\|^2$. Substituting them back to the previous equation, we can obtain the bound for the spectrum of $F \bar{\Phi}$:

$$m_f m_{\bar{\phi}} \leq \lambda \leq L_f L_{\bar{\phi}}. \quad (\text{C.2})$$

As a result, there exists a linear transformation $\zeta = Q\tilde{z}$, such that (C.1) is transformed to

$$\zeta_{k+1} = (I_d - \eta \Lambda) \zeta_k \quad (\text{C.3})$$

where Λ is a diagonal positive matrix whose elements are eigenvalues of $F \bar{\Phi}$, bounded by (C.2). Since system (C.3) shares the same form as the GD method applied to the quadratic convex function $\frac{1}{2} \zeta^T \Lambda \zeta$, the optimal stepsize and a tight convergence rate bound can be directly inferred from the analysis of GD method (Nesterov 2003, Theorem 2.1.14). Therefore, the optimal stepsize is given by $\eta = \frac{2}{L_f L_{\bar{\phi}} + \mu_f \mu_{\bar{\phi}}}$ and the tight convergence rate bound is $\rho = \frac{\kappa_f \kappa_{\bar{\phi}} - 1}{\kappa_f \kappa_{\bar{\phi}} + 1}$ for both (C.3) and its linear transformation (C.1).

D Matrices \hat{A} , \hat{B} , \hat{C} and \hat{D} in (40)

$$\hat{A} = \begin{bmatrix} A & & & & \\ B_{\Psi_{w,f}}^y C_1 & A_{\Psi_{w,f}} & & & \\ B_{\Psi_{w,\bar{\phi}}}^y C_2 & & A_{\Psi_{w,\bar{\phi}}} & & \\ B_{\Psi_{w,T}}^y C_3 & & & A_{\Psi_{w,T}} & \\ B_{\Psi_{w,\bar{\phi}}}^y C_4 & & & & A_{\Psi_{w,\bar{\phi}}} \\ B_{\Psi_{w,\bar{\phi}}}^y (C_2 - C_4) & & & & A_{\Psi_{w,\bar{\phi}}} \end{bmatrix}, \quad (\text{D.1})$$

$$\hat{B} = \begin{bmatrix} B_1 & B_2 & B_3 & B_4 \\ B_{\Psi_{w,f}}^y D_{11} + B_{\Psi_{w,f}}^u & B_{\Psi_{w,f}}^y D_{12} & B_{\Psi_{w,f}}^y D_{13} & B_{\Psi_{w,f}}^y D_{14} \\ B_{\Psi_{w,\bar{\phi}}}^y D_{21} & B_{\Psi_{w,\bar{\phi}}}^y D_{22} + B_{\Psi_{w,\bar{\phi}}}^u & B_{\Psi_{w,\bar{\phi}}}^y D_{23} & B_{\Psi_{w,\bar{\phi}}}^y D_{24} \\ B_{\Psi_{w,T}}^y D_{31} & B_{\Psi_{w,T}}^y D_{32} & B_{\Psi_{w,T}}^y D_{33} + B_{\Psi_{w,T}}^u & B_{\Psi_{w,T}}^y D_{34} \\ B_{\Psi_{w,\bar{\phi}}}^y D_{41} & B_{\Psi_{w,\bar{\phi}}}^y D_{42} & B_{\Psi_{w,\bar{\phi}}}^y D_{43} & B_{\Psi_{w,\bar{\phi}}}^y D_{44} + B_{\Psi_{w,\bar{\phi}}}^u \\ B_{\Psi_{w,\bar{\phi}}}^y (D_{21} - D_{41}) & B_{\Psi_{w,\bar{\phi}}}^y (D_{22} - D_{42}) + B_{\Psi_{w,\bar{\phi}}}^u & B_{\Psi_{w,\bar{\phi}}}^y (D_{23} - D_{43}) & B_{\Psi_{w,\bar{\phi}}}^y (D_{24} - D_{44}) - B_{\Psi_{w,\bar{\phi}}}^u \end{bmatrix}, \quad (\text{D.2})$$

$$\hat{C} = \begin{bmatrix} D_{\Psi_{s,f}}^y C_1 & & & & \\ D_{\Psi_{w,f}}^y C_1 & C_{\Psi_{w,f}} & & & \\ D_{\Psi_{s,\bar{\phi}}}^y C_2 & & & & \\ D_{\Psi_{w,\bar{\phi}}}^y C_2 & & C_{\Psi_{w,\bar{\phi}}} & & \\ D_{\Psi_{s,T}}^y C_3 & & & & \\ D_{\Psi_{w,T}}^y C_3 & & & C_{\Psi_{w,T}} & \\ D_{\Psi_{s,\bar{\phi}}}^y C_4 & & & & \\ D_{\Psi_{w,\bar{\phi}}}^y C_4 & & & & C_{\Psi_{w,\bar{\phi}}} \\ D_{\Psi_{s,\bar{\phi}}}^y (C_2 - C_4) & & & & \\ D_{\Psi_{w,\bar{\phi}}}^y (C_2 - C_4) & & & & C_{\Psi_{w,\bar{\phi}}} \end{bmatrix}, \quad (\text{D.3})$$

$$\hat{D} = \begin{bmatrix} D_{\Psi_{s,f}}^y D_{11} + D_{\Psi_{s,f}}^u & D_{\Psi_{s,f}}^y D_{12} & D_{\Psi_{s,f}}^y D_{13} & D_{\Psi_{s,f}}^y D_{14} \\ D_{\Psi_{w,f}}^y D_{11} + D_{\Psi_{w,f}}^u & D_{\Psi_{w,f}}^y D_{12} & D_{\Psi_{w,f}}^y D_{13} & D_{\Psi_{w,f}}^y D_{14} \\ D_{\Psi_{s,\bar{\phi}}}^y D_{21} & D_{\Psi_{s,\bar{\phi}}}^y D_{22} + D_{\Psi_{s,\bar{\phi}}}^u & D_{\Psi_{s,\bar{\phi}}}^y D_{23} & D_{\Psi_{s,\bar{\phi}}}^y D_{24} \\ D_{\Psi_{w,\bar{\phi}}}^y D_{21} & D_{\Psi_{w,\bar{\phi}}}^y D_{22} + D_{\Psi_{w,\bar{\phi}}}^u & D_{\Psi_{w,\bar{\phi}}}^y D_{23} & D_{\Psi_{w,\bar{\phi}}}^y D_{24} \\ D_{\Psi_{s,T}}^y D_{31} & D_{\Psi_{s,T}}^y D_{32} + D_{\Psi_{s,T}}^u & D_{\Psi_{s,T}}^y D_{33} + D_{\Psi_{s,T}}^u & D_{\Psi_{s,T}}^y D_{34} \\ D_{\Psi_{w,T}}^y D_{31} & D_{\Psi_{w,T}}^y D_{32} + D_{\Psi_{w,T}}^u & D_{\Psi_{w,T}}^y D_{33} + D_{\Psi_{w,T}}^u & D_{\Psi_{w,T}}^y D_{34} \\ D_{\Psi_{s,\bar{\phi}}}^y D_{41} & D_{\Psi_{s,\bar{\phi}}}^y D_{42} & D_{\Psi_{s,\bar{\phi}}}^y D_{43} & D_{\Psi_{s,\bar{\phi}}}^y D_{44} + D_{\Psi_{s,\bar{\phi}}}^u \\ D_{\Psi_{w,\bar{\phi}}}^y D_{41} & D_{\Psi_{w,\bar{\phi}}}^y D_{42} & D_{\Psi_{w,\bar{\phi}}}^y D_{43} & D_{\Psi_{w,\bar{\phi}}}^y D_{44} + D_{\Psi_{w,\bar{\phi}}}^u \\ D_{\Psi_{s,\bar{\phi}}}^y (D_{21} - D_{41}) & D_{\Psi_{s,\bar{\phi}}}^y (D_{22} - D_{42}) + D_{\Psi_{s,\bar{\phi}}}^u & D_{\Psi_{s,\bar{\phi}}}^y (D_{23} - D_{43}) & D_{\Psi_{s,\bar{\phi}}}^y (D_{24} - D_{44}) - D_{\Psi_{s,\bar{\phi}}}^u \\ D_{\Psi_{w,\bar{\phi}}}^y (D_{21} - D_{41}) & D_{\Psi_{w,\bar{\phi}}}^y (D_{22} - D_{42}) + D_{\Psi_{w,\bar{\phi}}}^u & D_{\Psi_{w,\bar{\phi}}}^y (D_{23} - D_{43}) & D_{\Psi_{w,\bar{\phi}}}^y (D_{24} - D_{44}) - D_{\Psi_{w,\bar{\phi}}}^u \end{bmatrix}. \quad (\text{D.4})$$